

Mirrors and Multilayers

T. Matsushita

Photon Factory

High Energy Accelerator Research Organization

outline

Mirrors

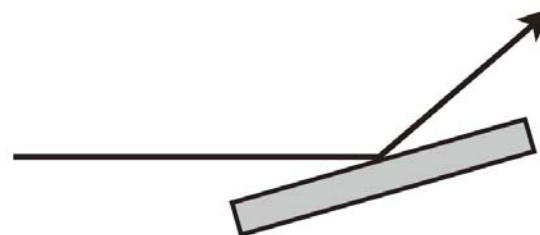
- (1) role of mirrors
- (2) refractive index and reflection of X-rays
- (3) mirror materials and mirror coatings
- (4) surface polishing and characterization
- (5) curved mirrors
- (6) transmission mirror
- (7) heat load and cooling

Multilayers

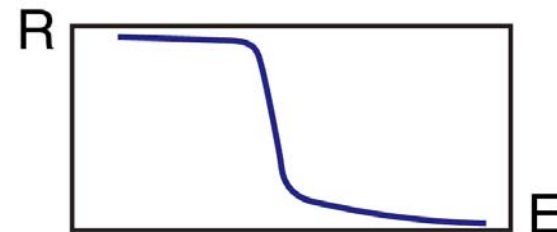
- (1) structure and X-ray reflectivity
- (2) fabrication
- (3) characterization
- (4) graded multilayers
- (5) applications

Mirrors

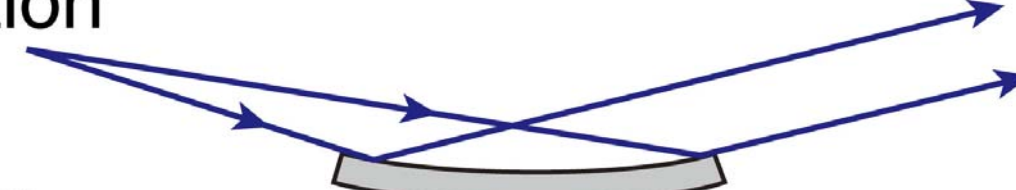
- Deflecting the beam



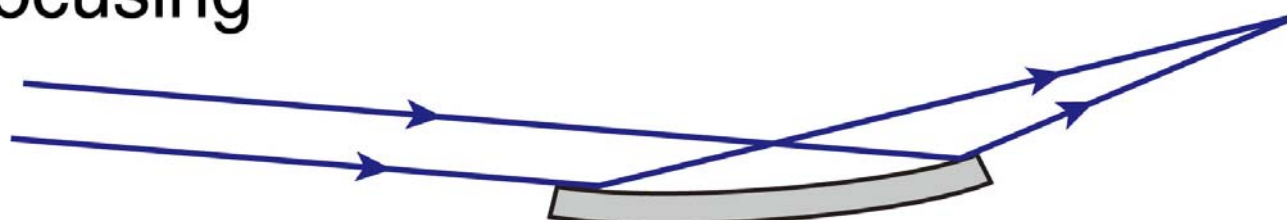
- Low pass filter



- Collimation



- Focusing



Refractive index

For X-rays, refractive index is slightly smaller than unity.

$$n = 1 - \delta + i\beta \quad \text{for} \quad E \propto \exp(+i(\omega t - kr))$$

$$(n = 1 - \delta - i\beta \quad \text{for} \quad E \propto \exp(-i(\omega t - kr)))$$

$$\delta = \frac{n_a r_e \lambda^2}{2\pi} f_1 \quad \beta = \frac{n_a r_e \lambda^2}{2\pi} f_2$$

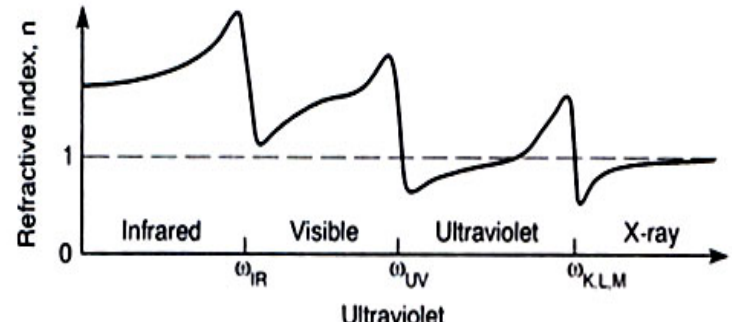
n_a : atomic density $r_e = \frac{e^2}{4\pi\epsilon_0 mc^2}$: (classical electron radius)

$$f_1 = f_0 + f' \quad f_2 = f''$$

f_0 : atomic scattering factor

f' and f'' : real and imaginary parts of anomalous dispersion term

For forward scattering, $f_0 = Z$



Refer to Chap. 3 of "soft X-rays and extreme ultraviolet radiation" by D. Attwood, Cambridge Univ. Press, 1999

	$\delta \times 10^5$	$\beta \times 10^7$
Si	0.488	0.744
Ge	0.908	2.33
Quartz	0.555	0.467
Pt	3.26	20.7
Au	2.96	19.5

Interaction of x-rays with matter

Experimental data

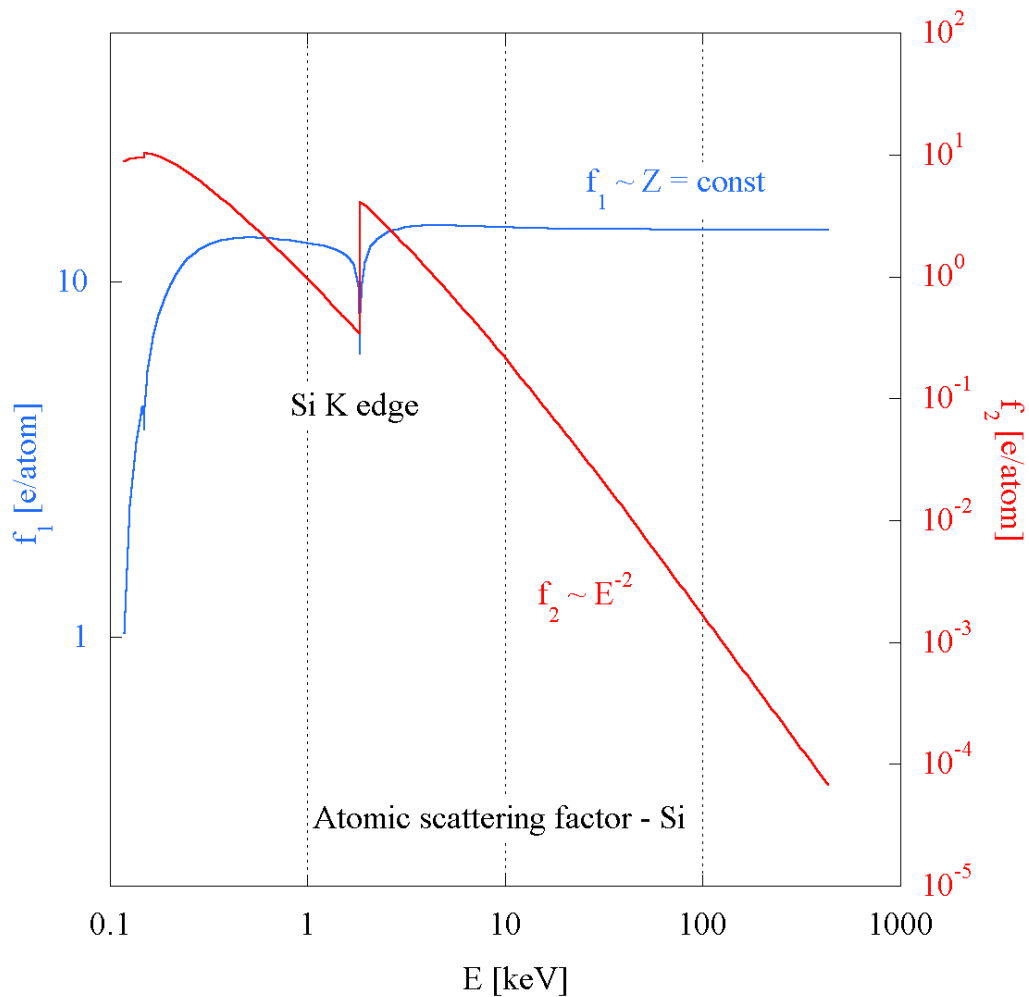
Asymptotic behaviour for $E > E(K)$:

$$f_1 \approx \text{const} \quad f_2 \approx 1/E^2$$

$$\delta \approx 1/E^2 \quad \beta \approx 1/E^4$$

$$\frac{\delta}{\beta} \approx E^2$$

High energy applications !



Snell's law

$$\frac{n_1}{n_2} = \frac{\cos(\theta_2)}{\cos(\theta_1)}$$

if $\frac{n_1}{n_2} \cos(\theta_1) = 1 \rightarrow \cos(\theta_2) = 1 \rightarrow \theta_2 = 0$

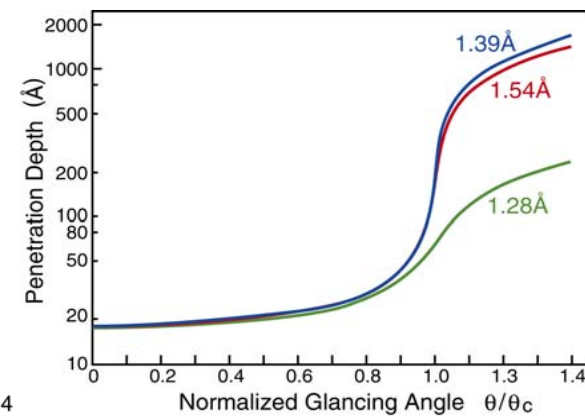
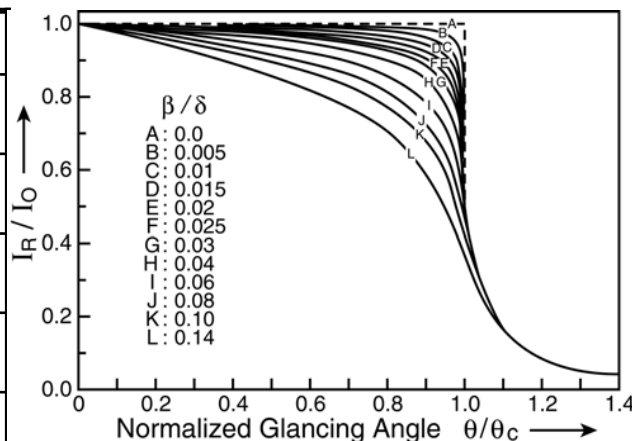
→ total external reflection

$$n_1 = 1 \text{ in vacuum} \rightarrow \cos(\theta_1) = 1 - \frac{\theta_1^2}{2} = n_2 = 1 - \delta$$

$$\theta_c = \sqrt{2\delta} \approx 1 \sim 20 \text{ mrad}$$

For 10 keV

	$\delta \times 10^5$	θ_c (degree)
Si	0.488	0.179
Ge	0.908	0.244
Quartz	0.555	0.191
Pt	3.26	0.463
Au	2.96	0.441



Reflection and refraction

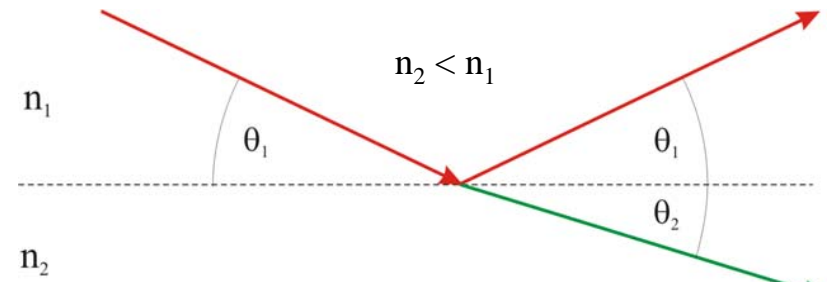
Fresnel formulae for reflection and transmission amplitudes

$$r_\sigma = \frac{n_1 \sin \theta_1 - n_2 \sin \theta_2}{n_1 \sin \theta_1 + n_2 \sin \theta_2}$$

$$r_\pi = \frac{n_1 \sin \theta_2 - n_2 \sin \theta_1}{n_1 \sin \theta_2 + n_2 \sin \theta_1}$$

$$t_\sigma = \frac{2n_1 \sin \theta_1}{n_1 \sin \theta_1 + n_2 \sin \theta_2}$$

$$t_\pi = \frac{2n_1 \sin \theta_2}{n_1 \sin \theta_2 + n_2 \sin \theta_1}$$



Reflectivity amplitude as a function of external angle of incidence θ (vacuum)

$$r_\sigma = \frac{\sqrt{n_1^2 - \cos^2 \theta} - \sqrt{n_2^2 - \cos^2 \theta}}{\sqrt{n_1^2 - \cos^2 \theta} + \sqrt{n_2^2 - \cos^2 \theta}}$$

$$r_\pi = \frac{n_1/n_2 \sqrt{n_2^2 - \cos^2 \theta} - n_2/n_1 \sqrt{n_1^2 - \cos^2 \theta}}{n_1/n_2 \sqrt{n_2^2 - \cos^2 \theta} + n_2/n_1 \sqrt{n_1^2 - \cos^2 \theta}}$$

Including graded interfaces (Gaussian density gradient, phase shift)

$$r = r_{ideal} \cdot e^{-\frac{8\pi^2}{\lambda^2} \sqrt{n_1^2 - \cos^2 \theta} \sqrt{n_2^2 - \cos^2 \theta} \sigma^2}$$

Reflectivity formula

$$R = \frac{(\theta - A)^2 + B^2}{(\theta + A)^2 + B^2}$$

$$A = \sqrt{\frac{(a^2 + b^2)^{1/2} + a}{2}}$$

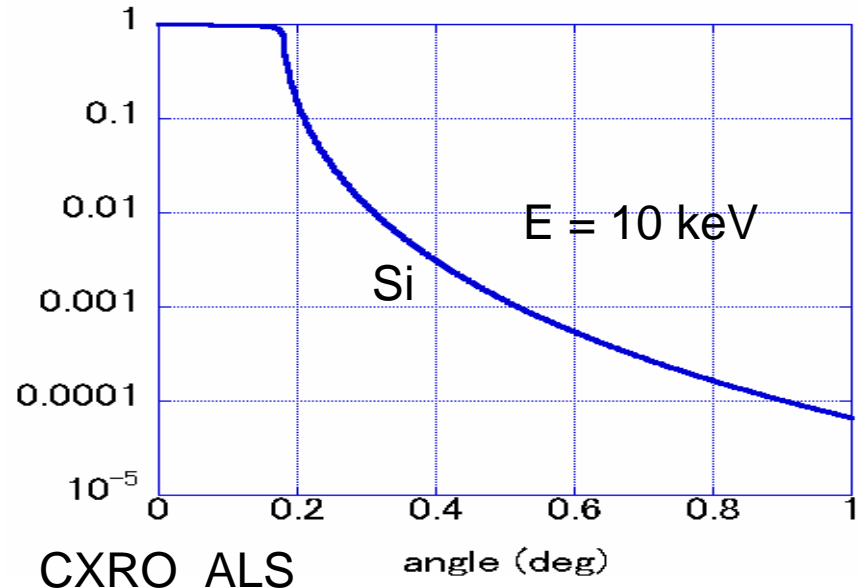
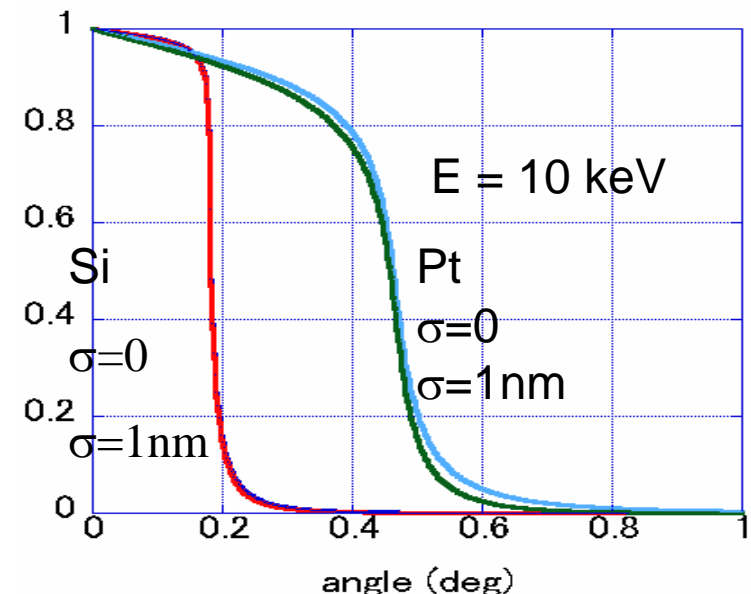
$$B = \sqrt{\frac{(a^2 + b^2)^{1/2} - a}{2}}$$

$$a = \theta^2 - \theta_c^2 = \theta^2 - 2\delta \quad \quad b = 2\beta$$

$$q = 4\pi \frac{\sin(\theta)}{\lambda}$$

For $q >> q_c$

$$R \propto \frac{1}{q^4}$$

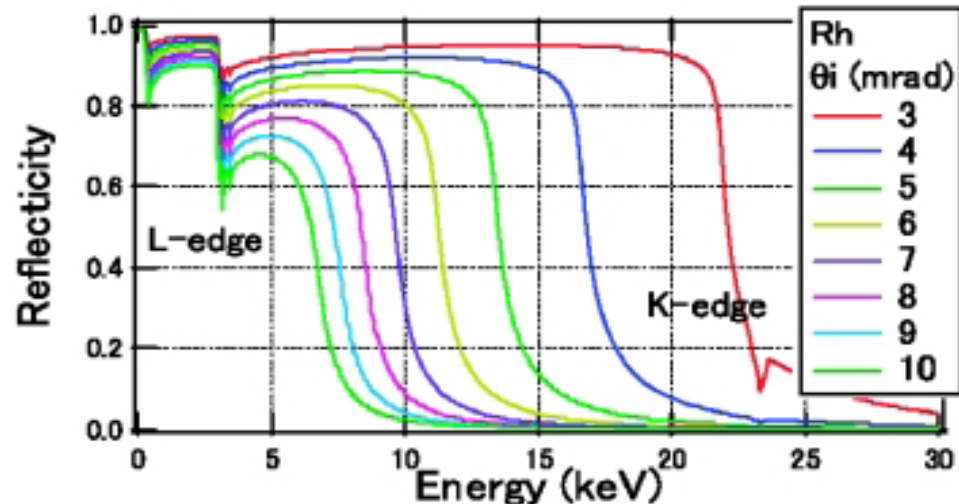


H. **Compton** and S. K. **Allison**, X-Rays in Theory and Experiment (D. Van Nostrand Company, Inc., New York, 1935),

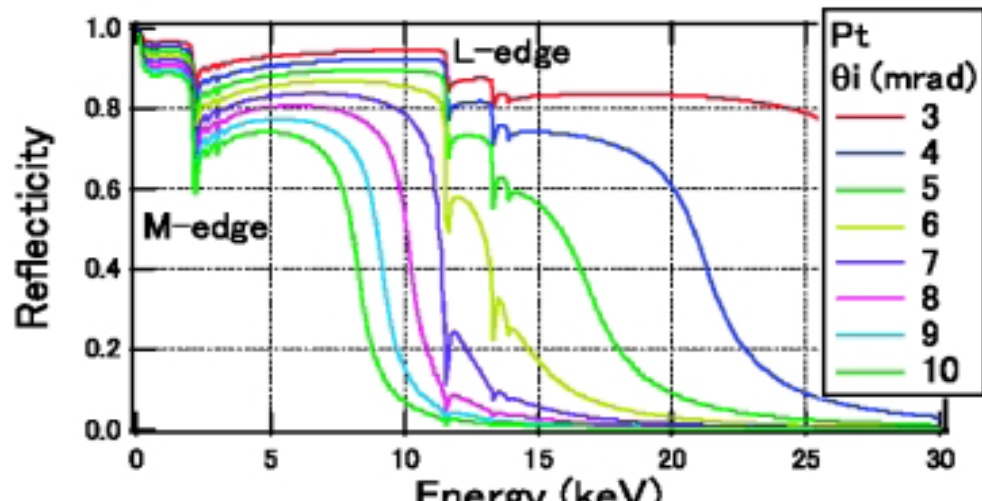
“X-ray Interactions with Matter”
http://henke.lbl.gov/optical_constants/

Reflectivity curve

A total reflection mirror works as a low-pass energy filter. The cut-off energy can be controlled by selecting the material and the glancing angle.



(a)



(b)

From Uruga & Nomura, Hoshako(放射光) 2006 vol.19 No.4 pp.248-257, Fig.3

Requisites for mirror materials

- (1) Can be polished to a smooth and accurate surface figure.
- (2) Large material available. (~1.4 m long mirror presently used)
- (3) Mechanically hard, Radiation resistive
- (4) Good thermal conductivity, low thermal dilation constant
- (5) No (low) gas emission under X-ray irradiation
- (6) Can be bent.
- (7) Reasonable cost (material itself and fabrication)

Important parameters

- Surface figure
flat, cylindrical, elliptic, parabolic, spherical, toroidal,
ellipsoidal, paraboloidal,----
- Roughness
root-mean-square roughness ~0.1 nm
- Slope error
root-mean-square slope ~0.5 μ rad
- Thermal property
thermal conductivity
dilation constant
- Absorption edges X-ray absorption

Materials for mirrors

Silicon

Zerodur

Fused silica

GlidCop (alumina dispersion strengthened copper alloys)

Cu with electroless Ni layer

Silicon Carbide (CVD)

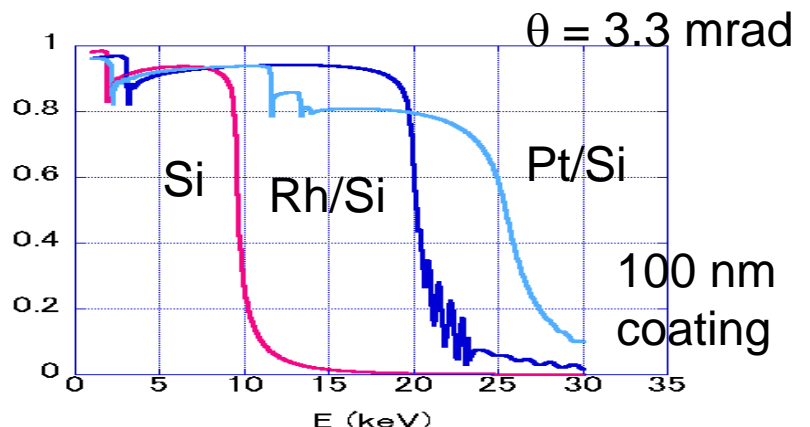
Materials for mirror coating

Desired critical energy with a given glancing angle

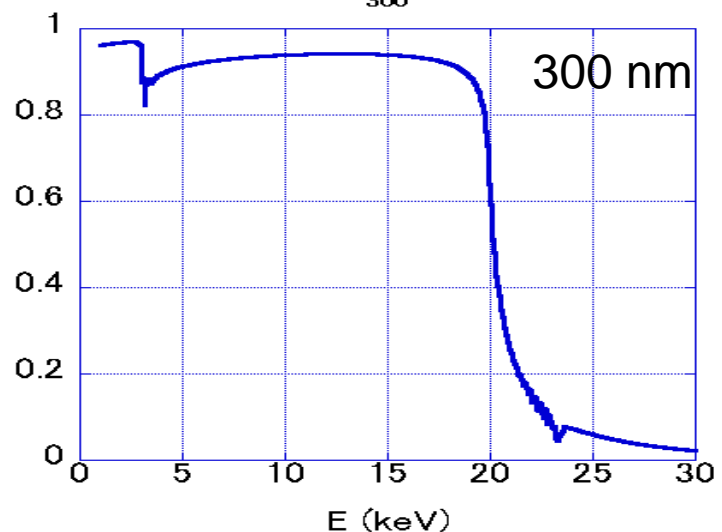
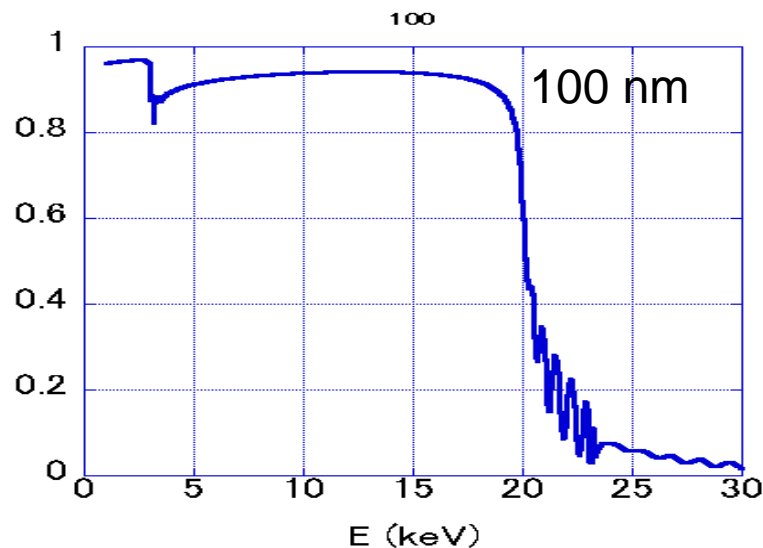
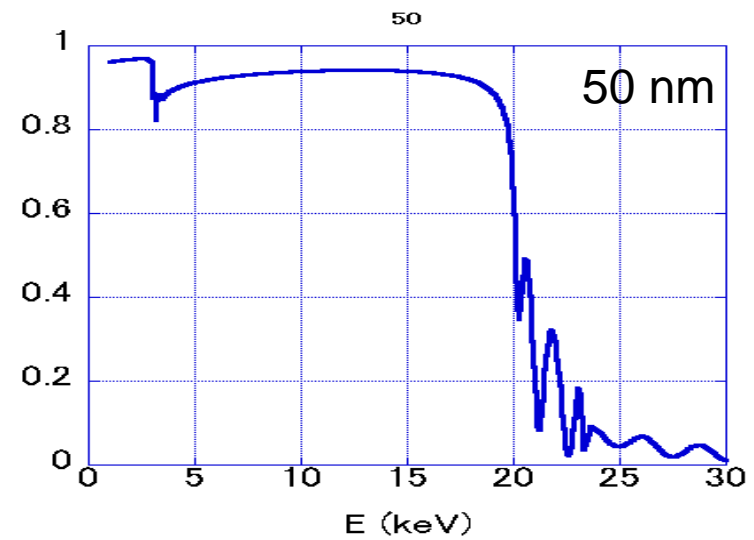
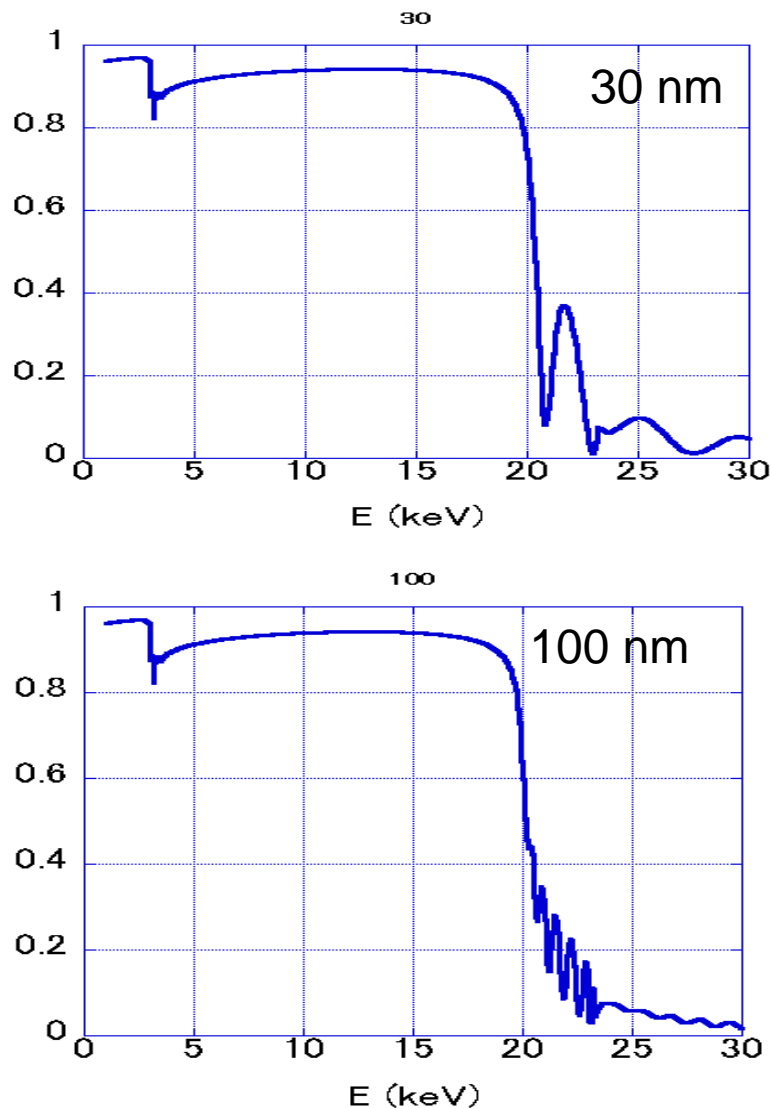
Retain smooth surface

No absorption edges desirable in the required energy range

Au, Pt, Rh, Ni, Pd, Ru

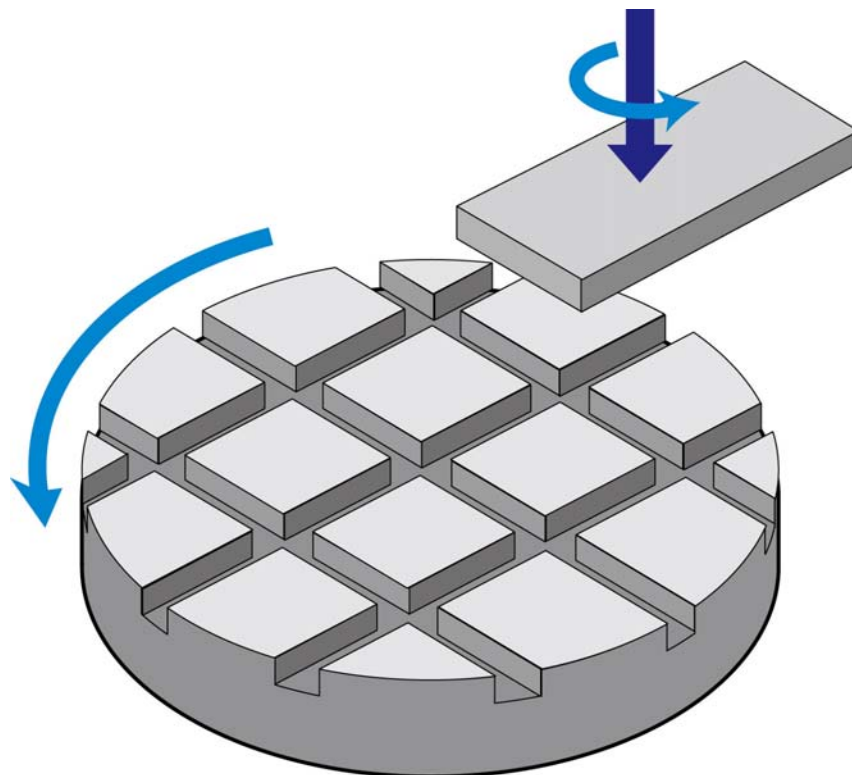


Coating of mirrors (Rh coating on silicon)



Fabrication of mirrors

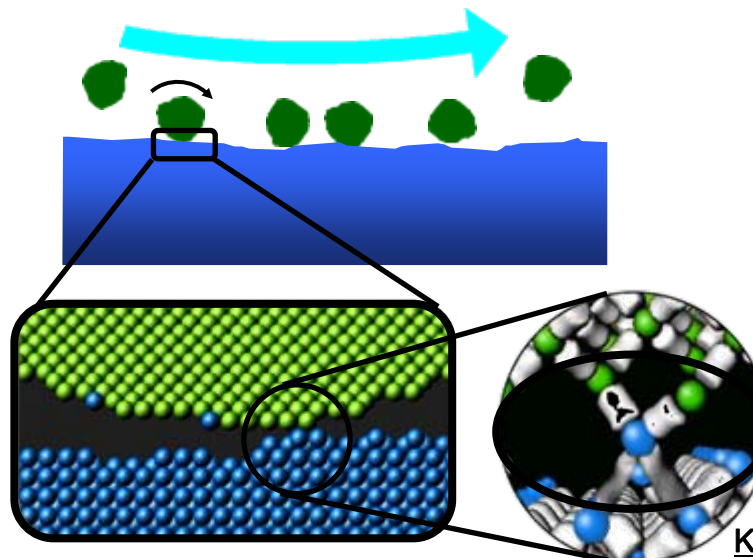
- Grinding
- Diamond turning
- Lapping
- polishing



Advanced Polishing Technique (Elastic Emission Machining)

In EEM, chemical reaction between solid surfaces is utilized.

Ultrafine powder particles having reactivity to the work surface are employed.

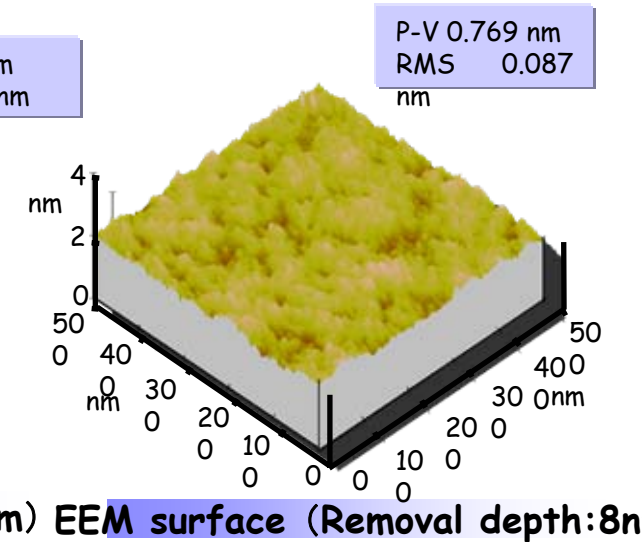
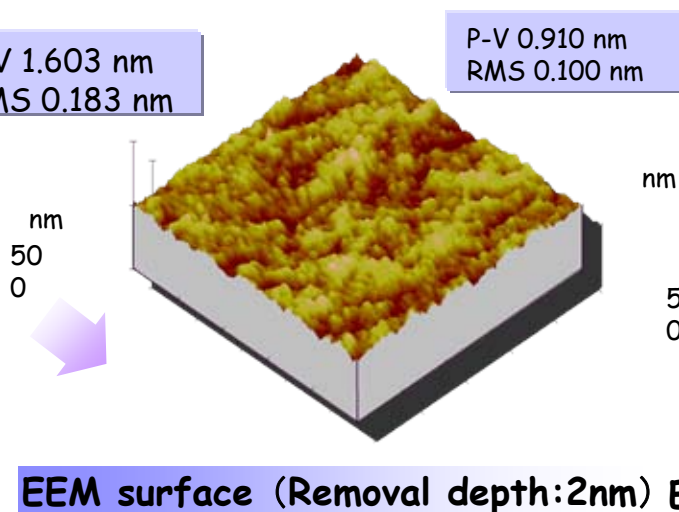
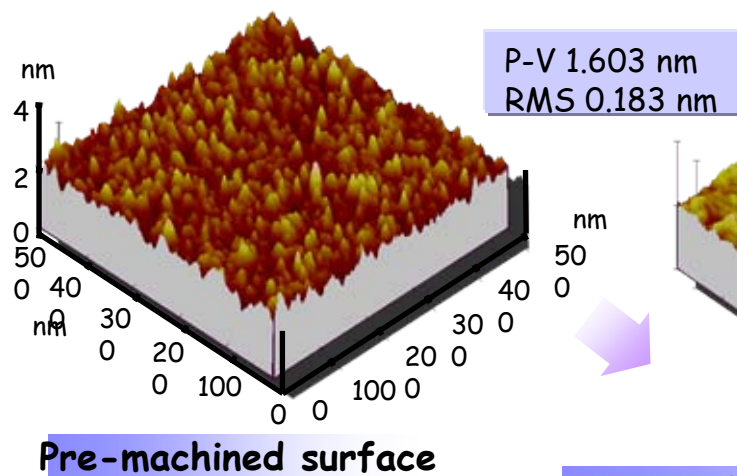


Ultra-fine particles are supplied to the work surface by ultrapure water flow.

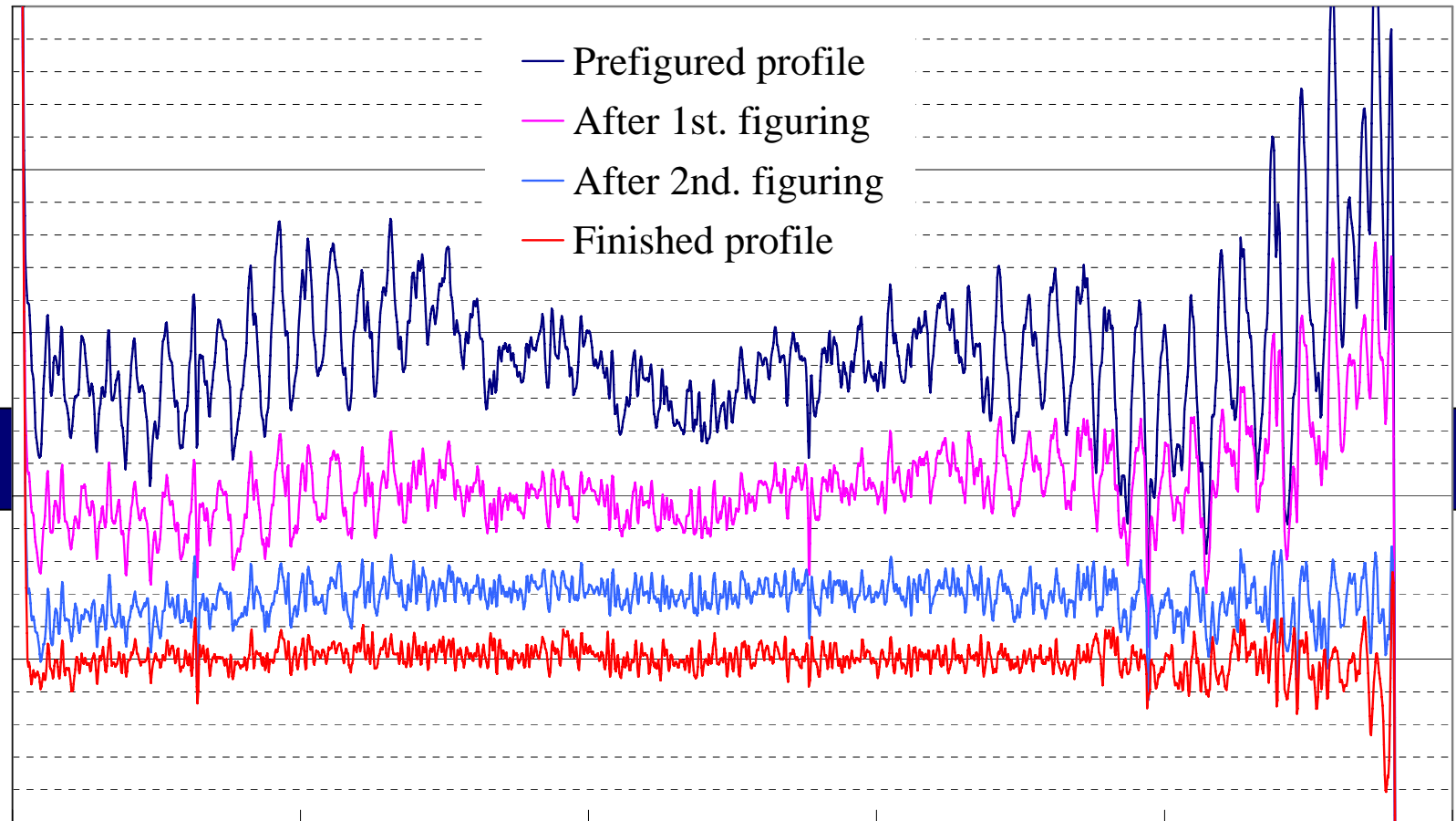
Atom removal occurs selectively at the topmost site of the work surface.

K. Yamauchi, et al.

Rev. Sci. Instrum., 73, (2002), pp. 4028-4033

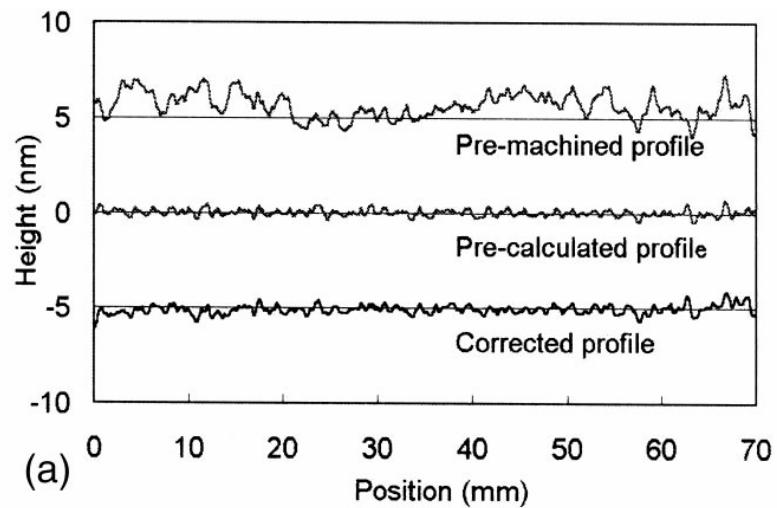


Typical figuring properties using EEM



H. Mimura et al., Rev. Sci. Instrum., 76, 045102 (2005).

K. Yamauchi et al., Rev. Sci. Instrum., 74 (5), 2894-2898 (2003).



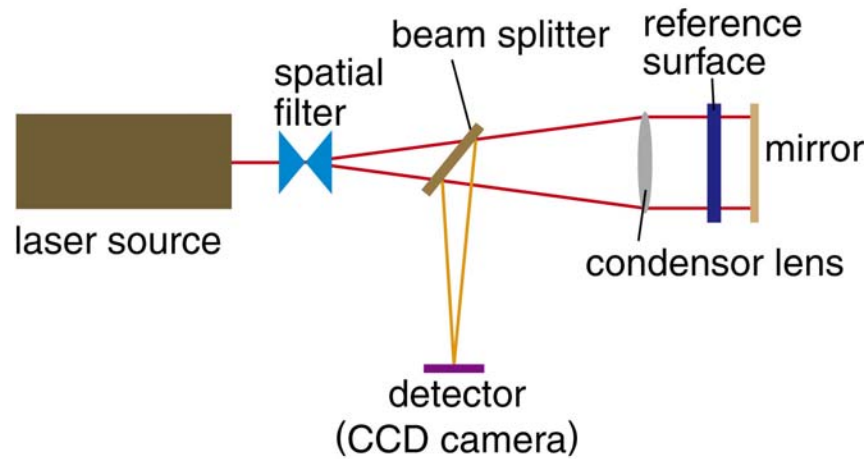
X-ray image reflected at figure corrected area
(15% of the total area on each side is not figure-corrected)



(b) X-ray image reflected at noncorrected area

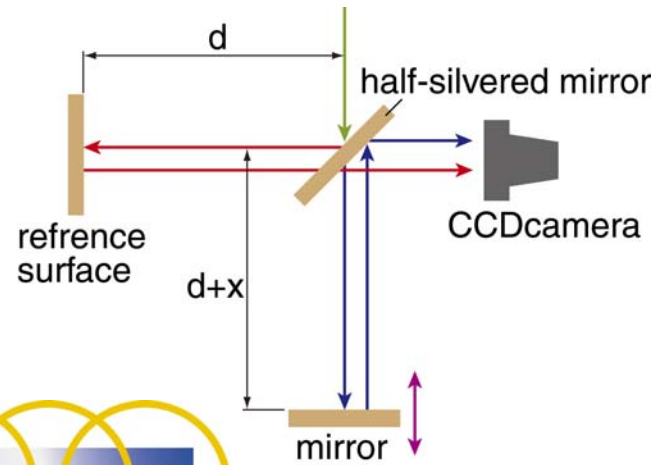
Characterization of mirrors (surface roughness and figure)

Fizeau interferometer

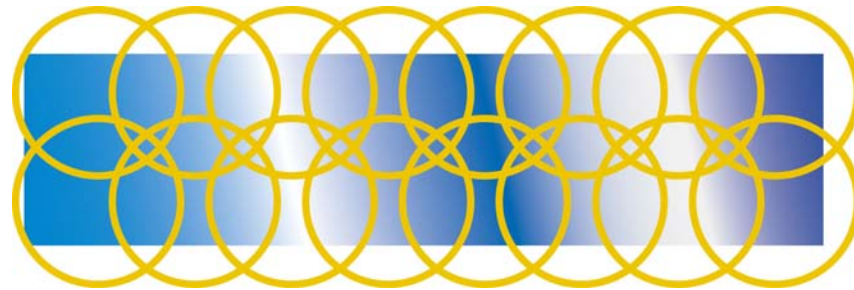


Michelson interferometer

Twyman-Green interferometer
(mirror: rotatable, point source)



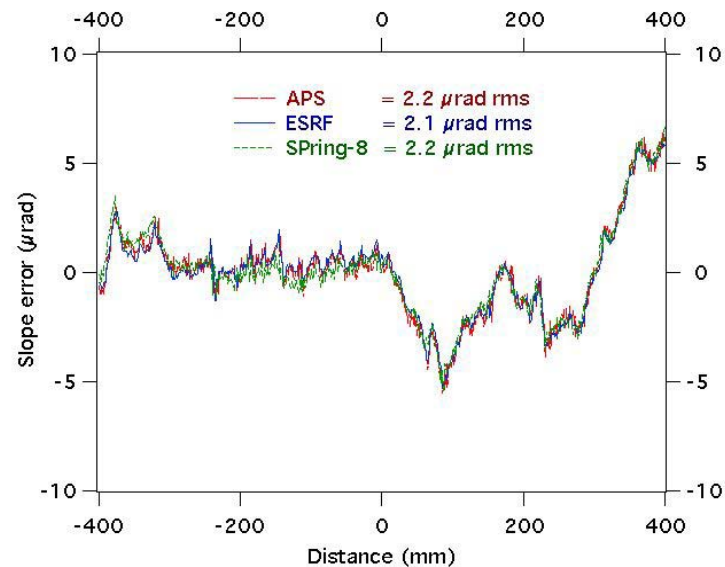
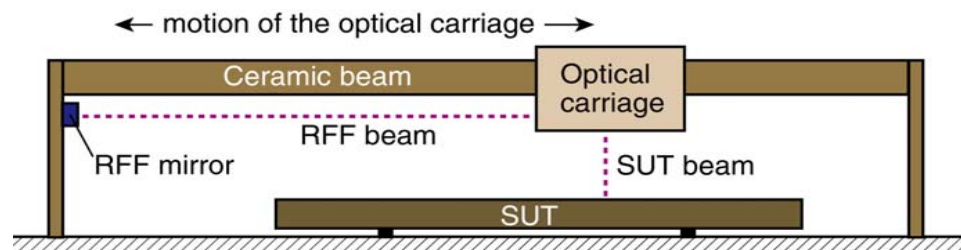
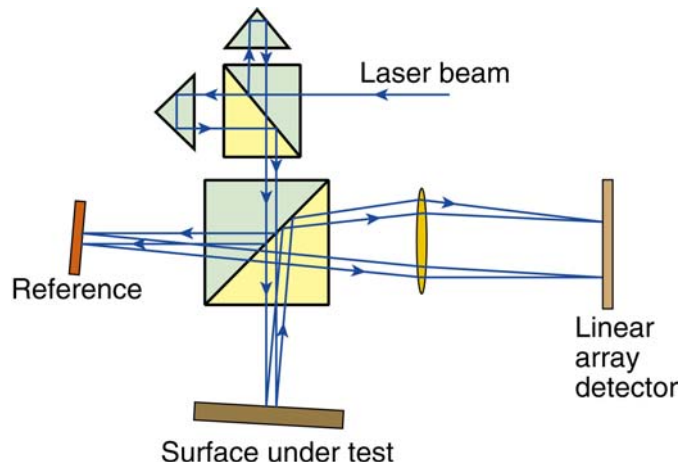
Stitching interferometry



Atomic Force Microscopy
Stylus measurement

Characterization of mirrors (slope errors)

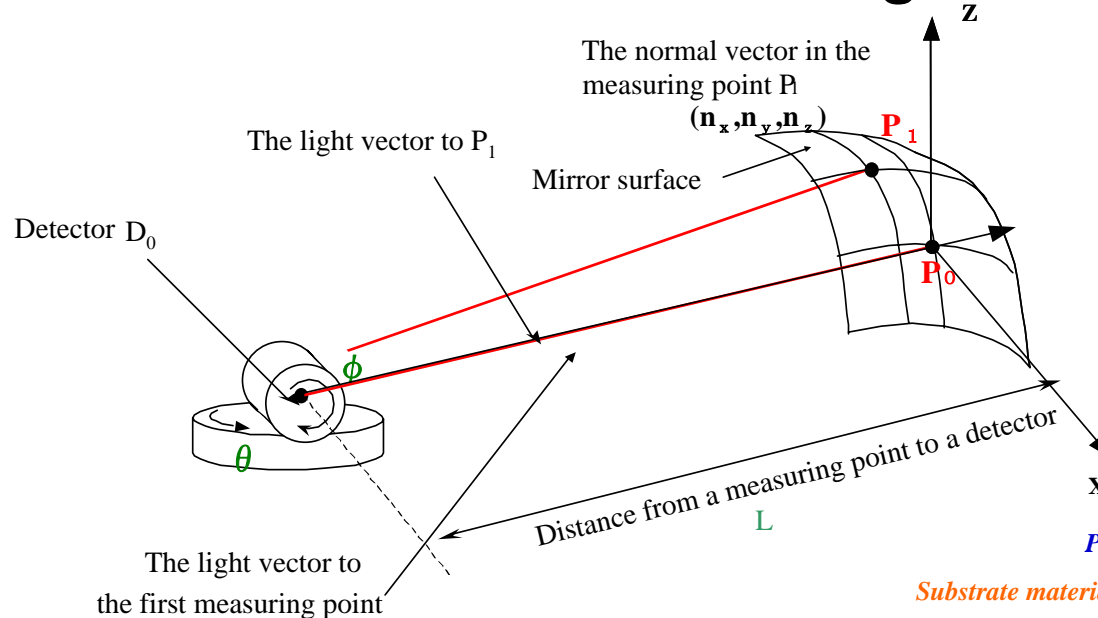
- Long Trace Profiler



"Results of x-ray mirror round robin metrology measurements at the APS, ESRF, and SPring-8 optical metrology laboratories"
L. Assoufid, A. Rommevaux, H. Ohashi, K. Yamauchi, H. Mimura, J. Qian, O. Hignette, T. Ishikawa, C. Morawe, A. Macrander, A. Khounsary, S. Goto
SPIE Conference on Optics and Photonics, San Diego: SPIE Proc. 5921-21, 129 (2005).

Characterization of mirrors (slope errors)

Surface Gradient Integrated Profiler



Y. Higashi et. al. , Proc. SPIE,
OPTICS&PHOTONICS,
Advances in Metrology for X-Ray
and EUV Optics, 5921-07, San
Diego, CA, USA, 31 July-4
August, (2005)

Basic Principle

The normal vectors at each points on the surface are determined by making the incident light beam on the mirror surface and the reflected beam at that point coincide.

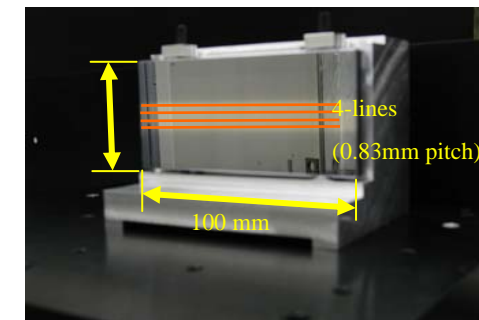
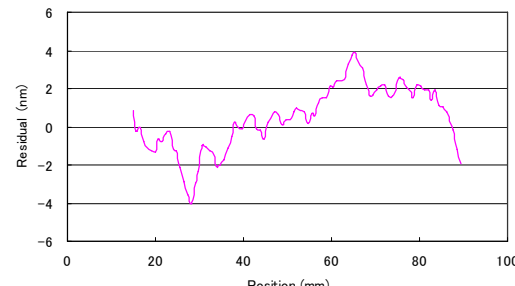


Surface gradient at each point is calculated from the normal vector and the surface profile is obtained by integrating the gradients.

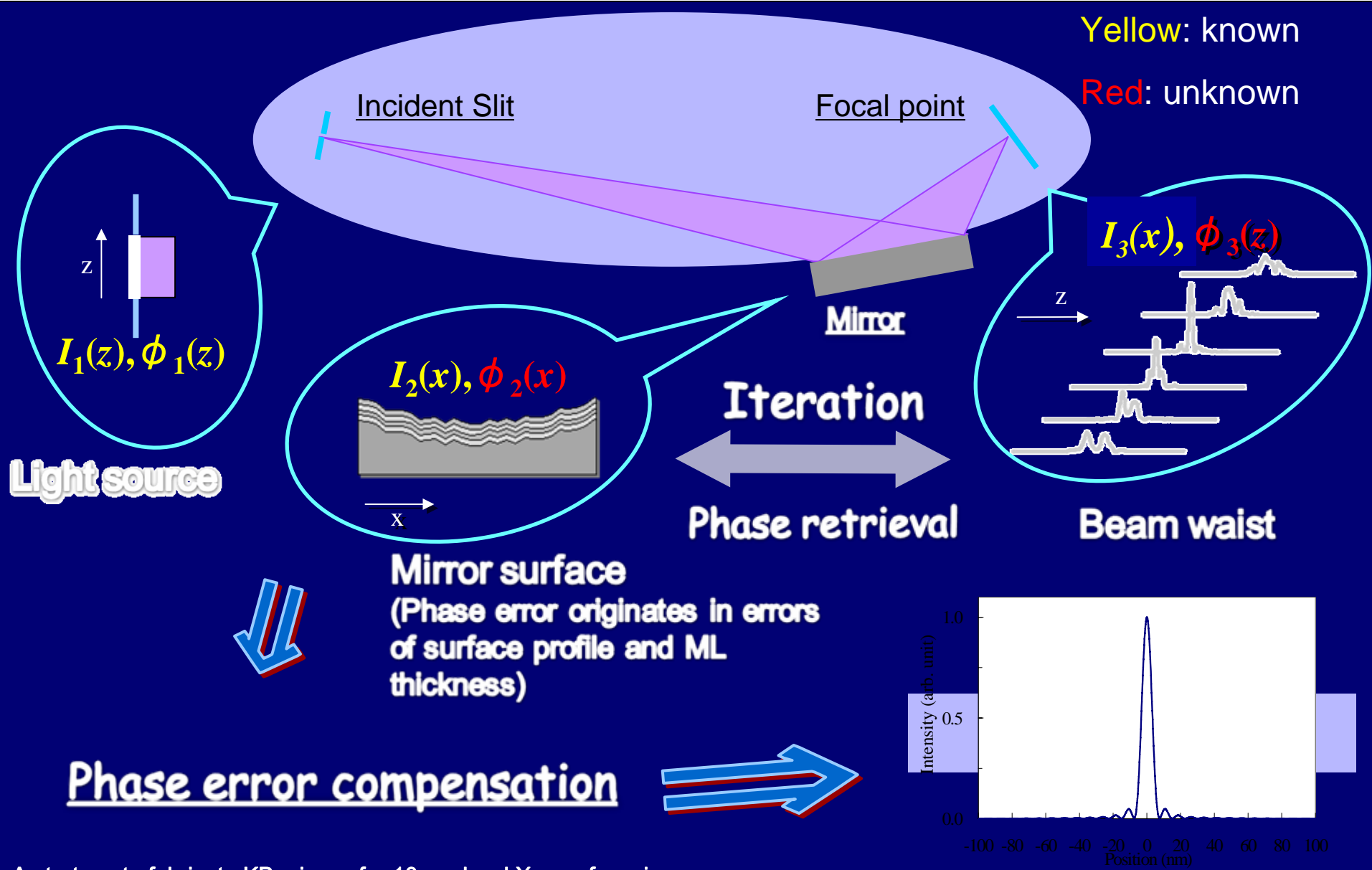
Parameters of the mirror

Substrate material	CZ(111)Si single crystal
Surface coating	Pt
Effective mirror size	100 mm
In longitudinal direction	
Length of ellipse	500.075 m
Breadth of ellipse	44.7 mm

Differential surface profile between RADSI and present instrument



At-wavelength phase-retrieval interferometry

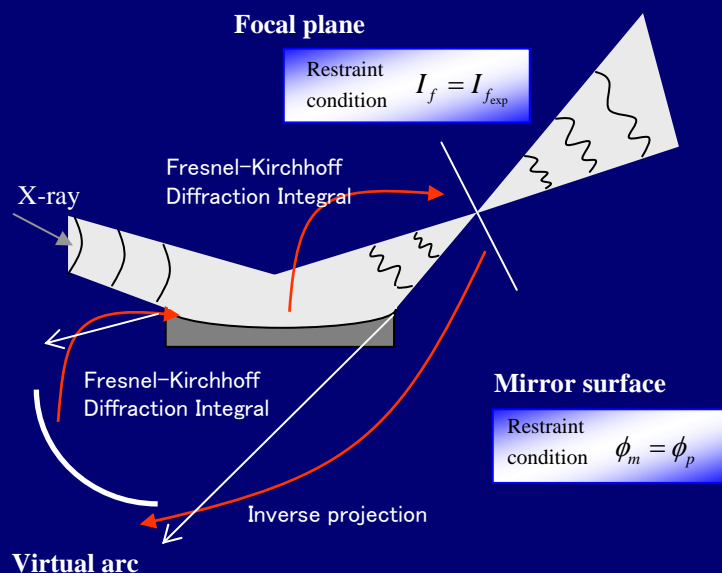


A strategy to fabricate KB mirrors for 10 nm hard X-rays focusing,

K. Yamauchi, X-Ray Optics: A Roadmap for the Next 10 Years

A one-day (August 1, 2005) Workshop at SPIE's Optics & Photonics 2005 San Diego, California USA

Phase retrieval properties



On focal plane

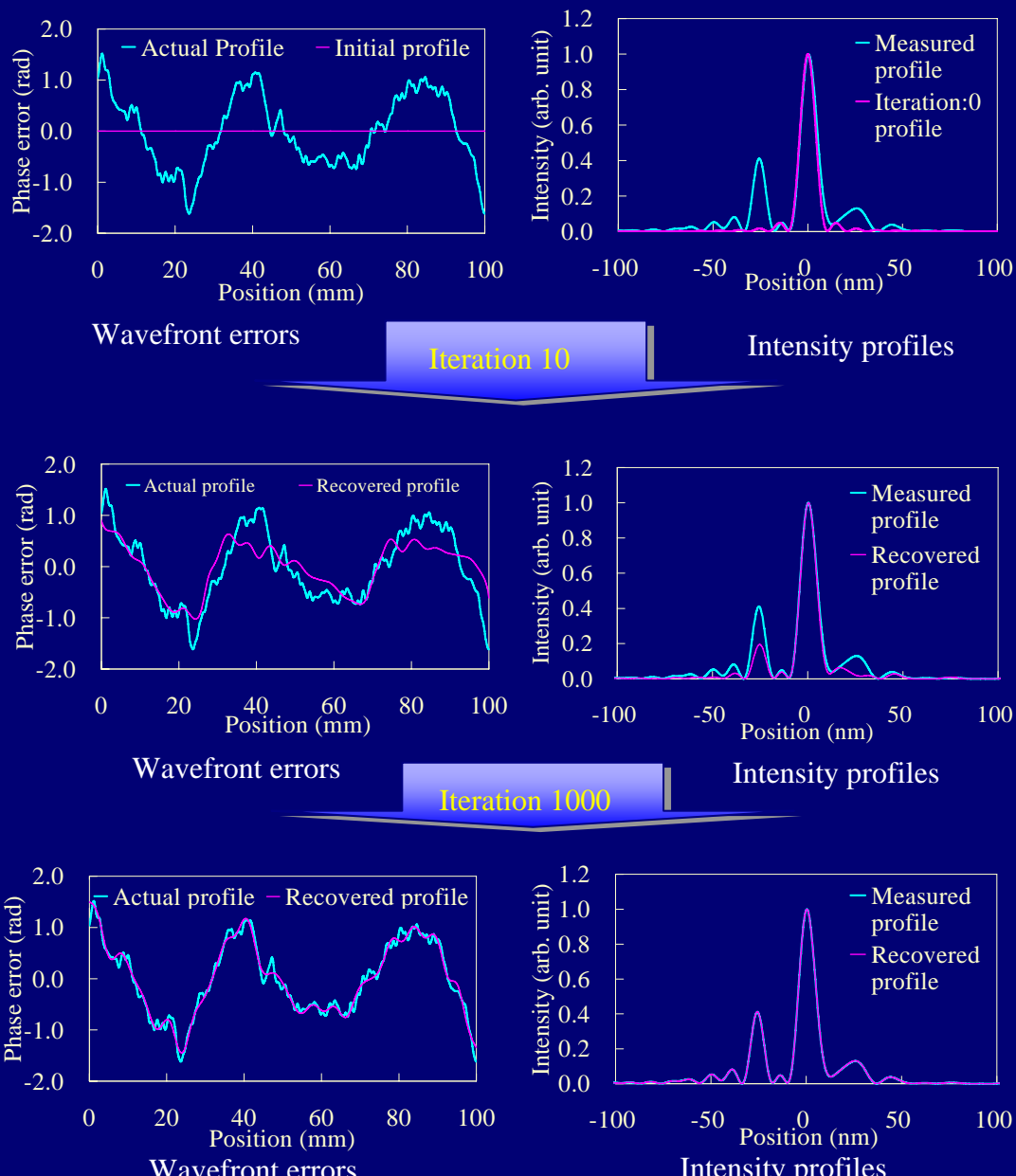
Intensity is changed to experimental value.

Phase is kept to be recovered value.

On mirror surface

Intensity is changed to theoretical value.

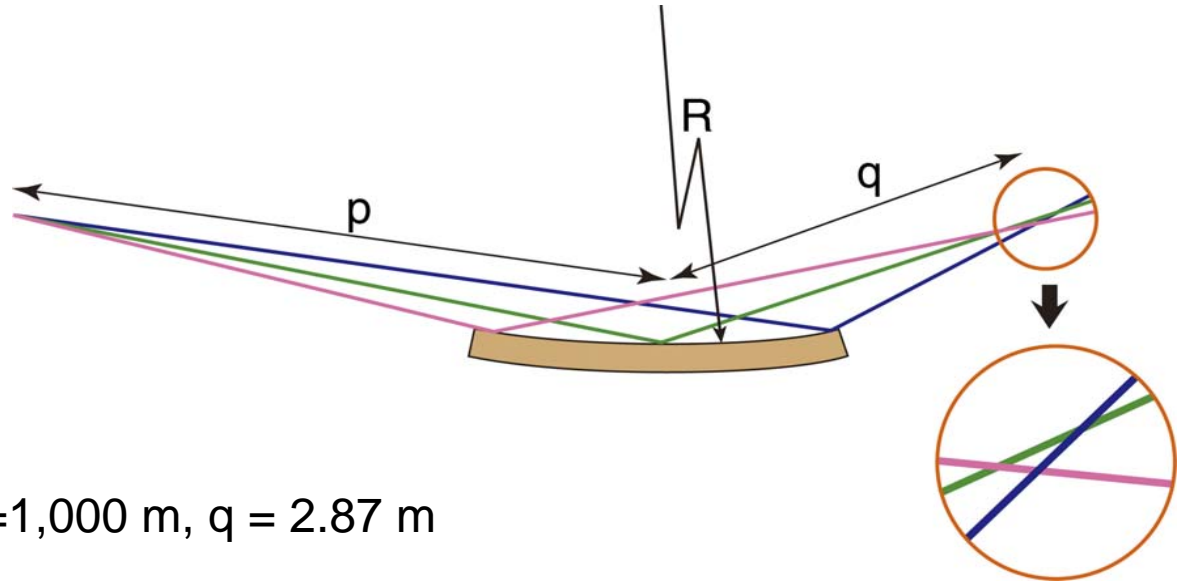
Phase is kept to be recovered value.



curved mirrors (focusing, collimating)

Cylindrical mirror

$$\frac{1}{p} + \frac{1}{q} = \frac{2}{R \sin(\theta)}$$

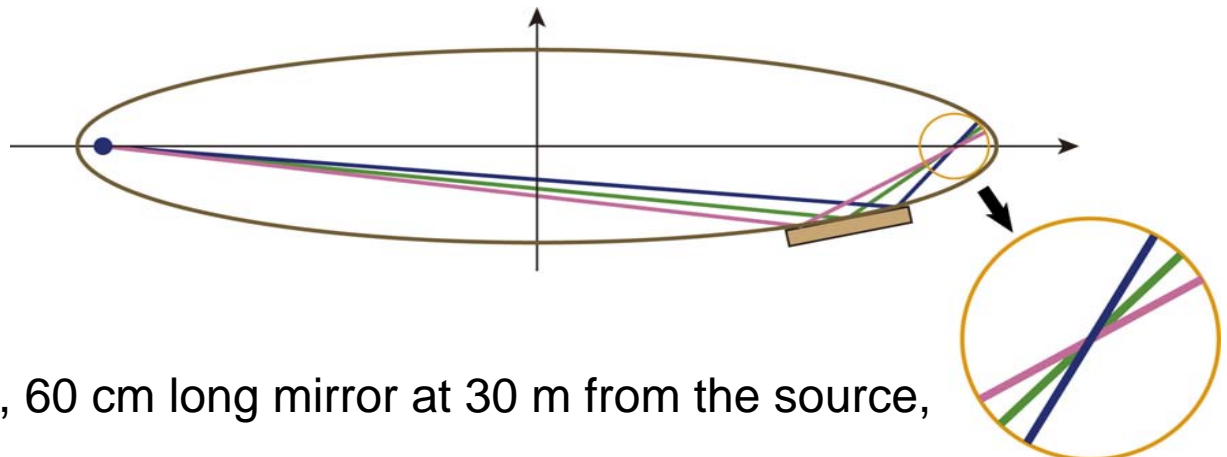


$$P=30 \text{ m}, \theta = 0.3^\circ, R=1,000 \text{ m}, q = 2.87 \text{ m}$$

$$R=100 \text{ m}, q = 0.26 \text{ m}$$

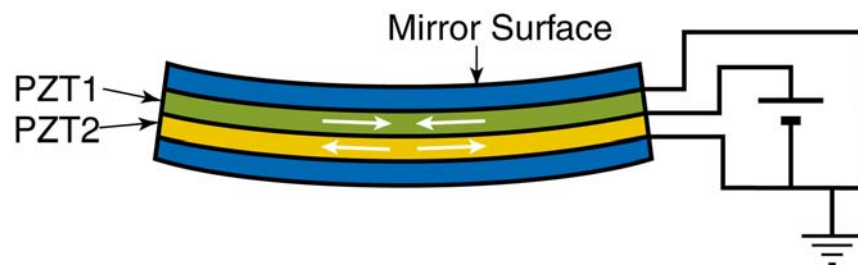
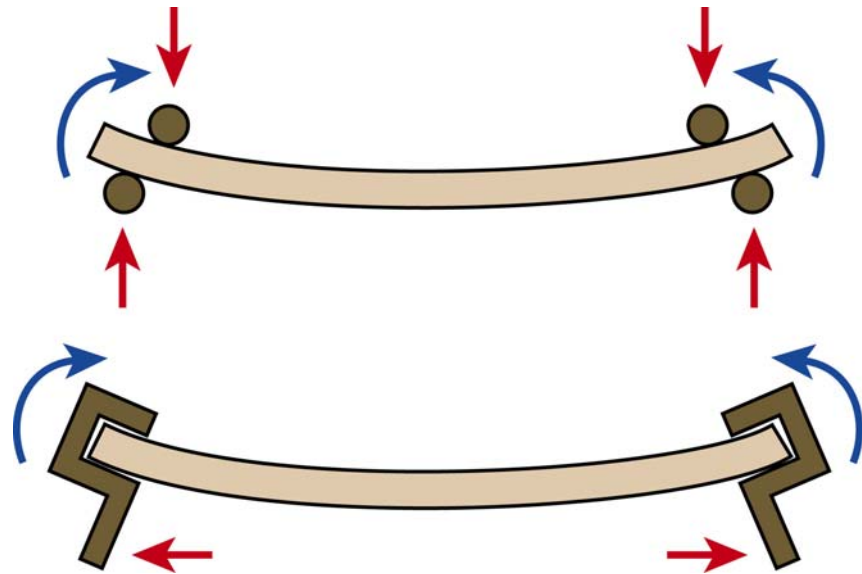
Elliptic mirror

$$\frac{x^2}{a^2} + \frac{y^2}{b^2} = 1$$

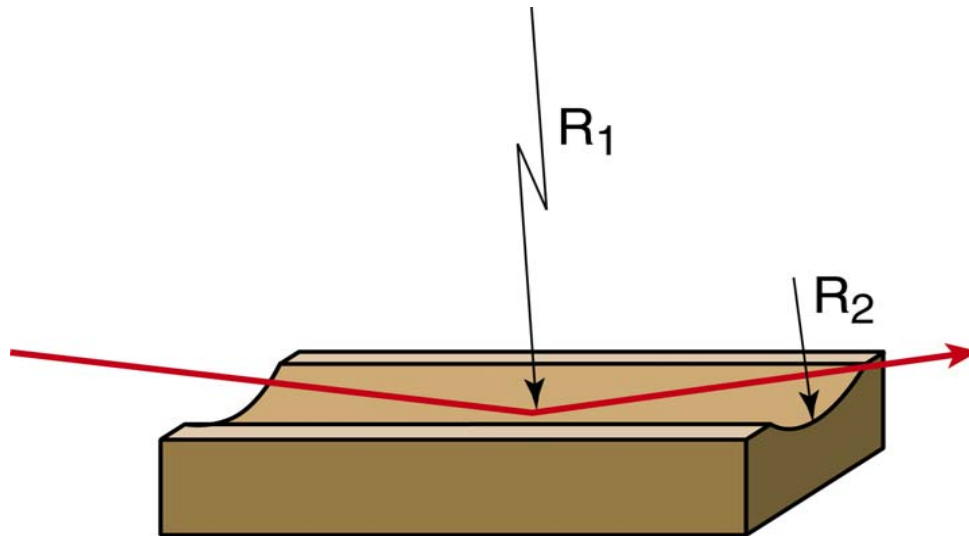


$$a = 15.5 \text{ m}, b = 0.03 \text{ m}, 60 \text{ cm long mirror at } 30 \text{ m from the source}, \\ \theta \sim 0.28^\circ - 0.37^\circ, q = 1 \text{ m}$$

Bending mechanisms

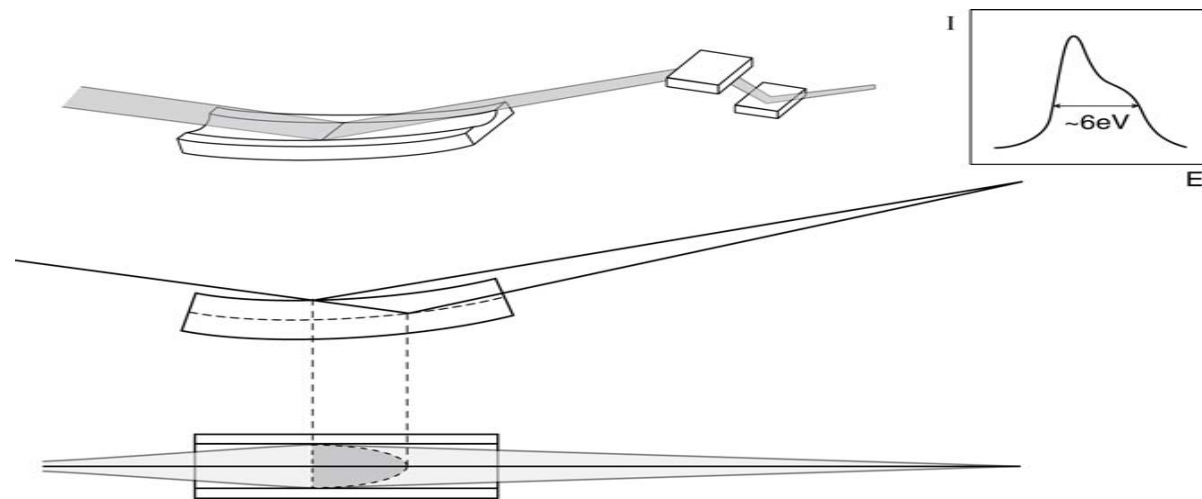


bent-cylinder, toroidal mirror



$$R_1 = \frac{2pq}{(p+q)\sin(\theta)}$$

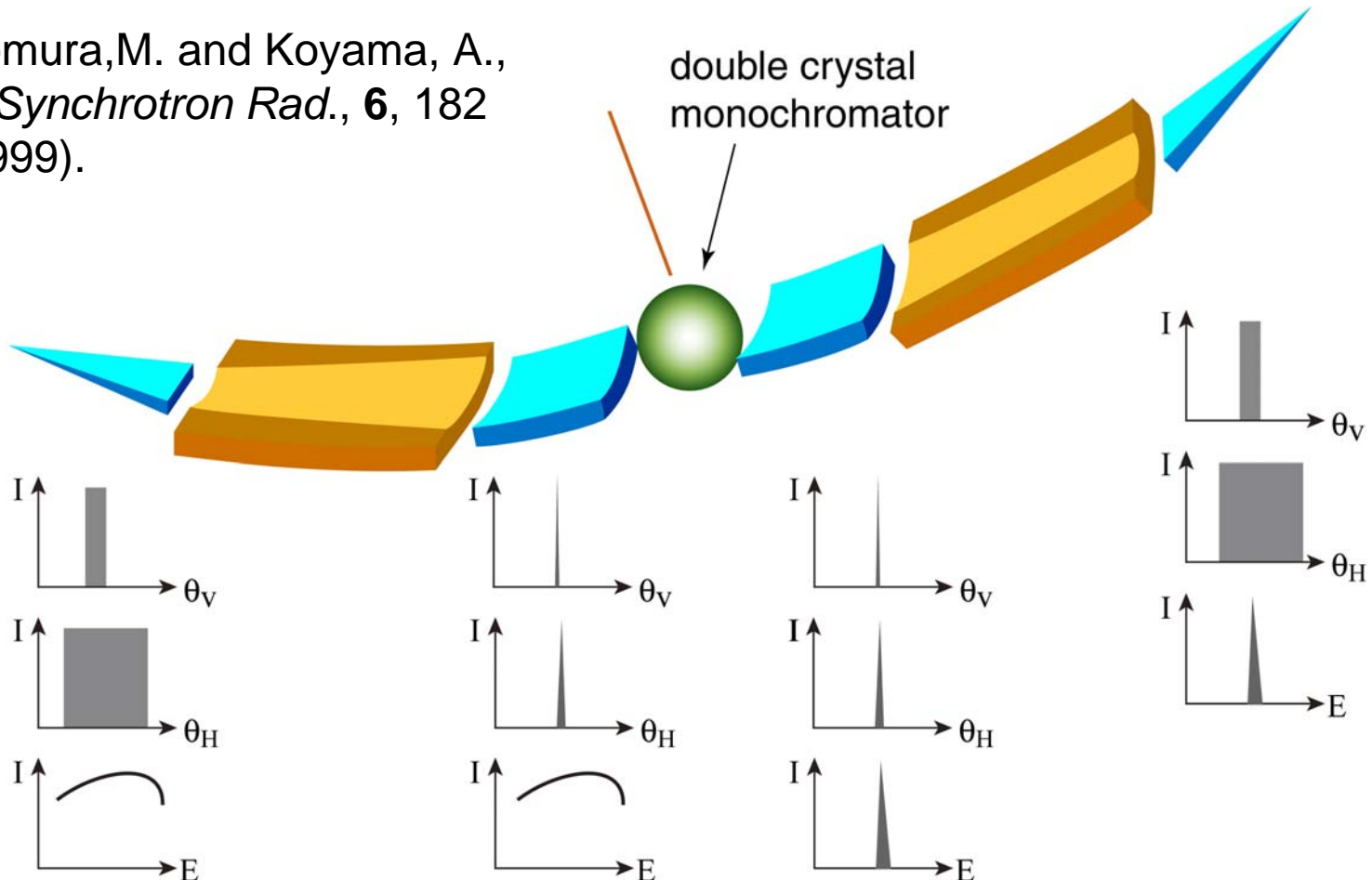
$$R_2 = \frac{{R_1}^2}{\sin^2 \theta}$$



bent conical mirror

– approximation to paraboloidal mirror –

Nomura,M. and Koyama, A.,
J. Synchrotron Rad., **6**, 182
(1999).



Kirkpatrick-Baez (KB) optics for nanometer focusing

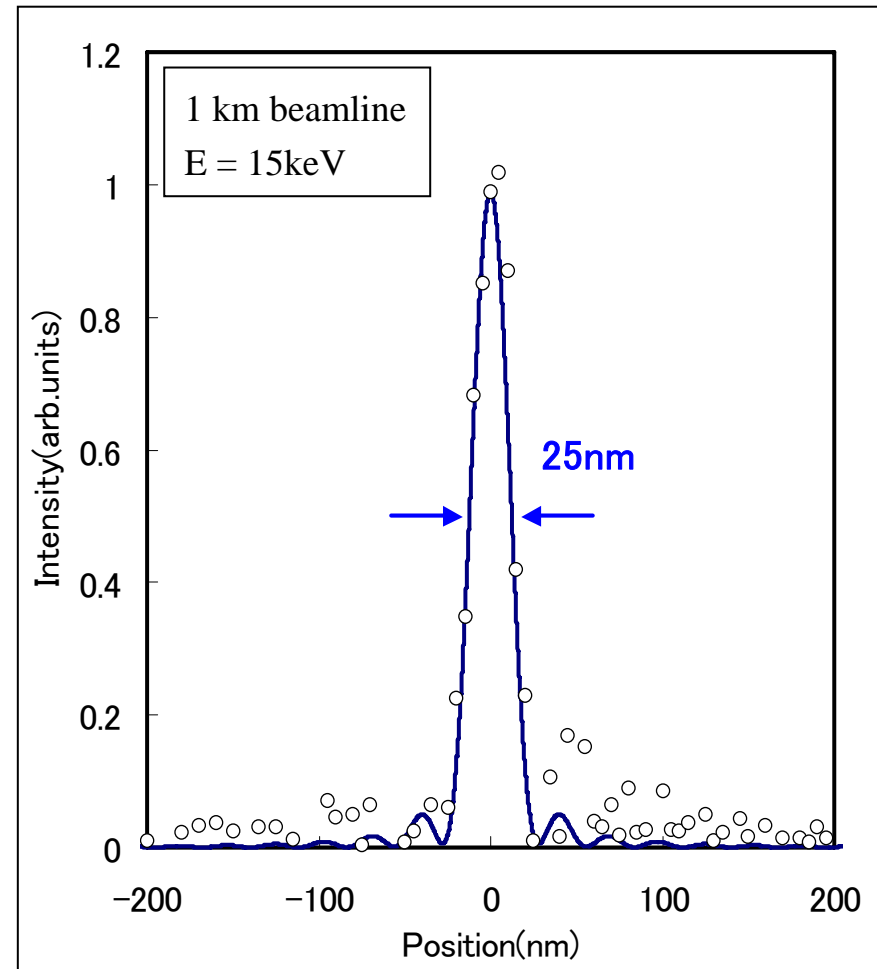
P. Kirkpatrick, A.V. Baez, J. Opt. Soc. Am. 38, 766 (1948)

Spring-8/Osaka KB development

- Static and figured Si substrates
- Plasma Chemical Vapour Machining (PCVM)
- Elastic Emission Machining (EEM)
- Pt coating + thickness correction
- Focal spots below 30 nm
- Aiming less than 10 nm using multilayers



[23] H. Mimura et al,
Jpn. J. Appl. Phys. Part 2 44, 18539 (2005)

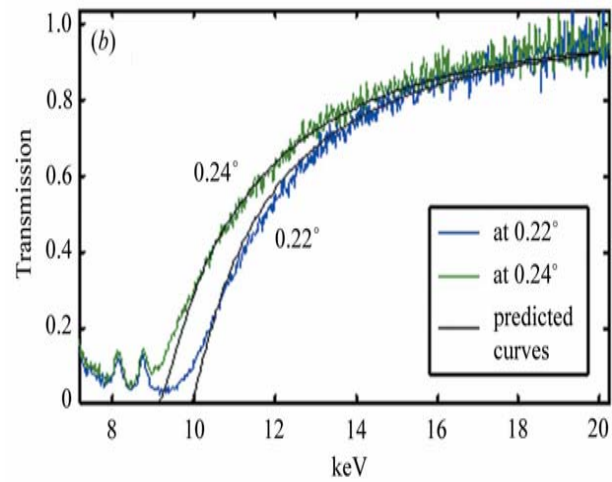
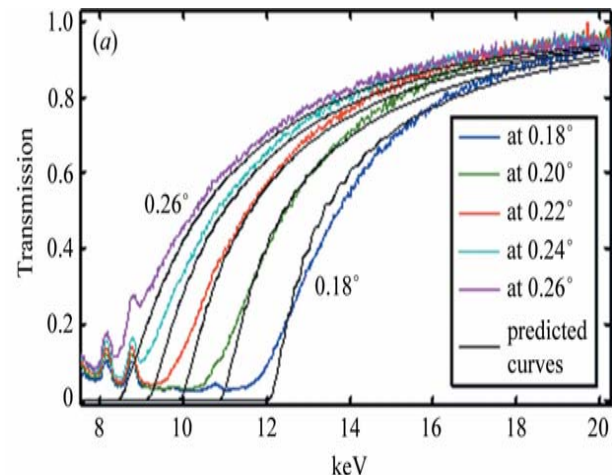
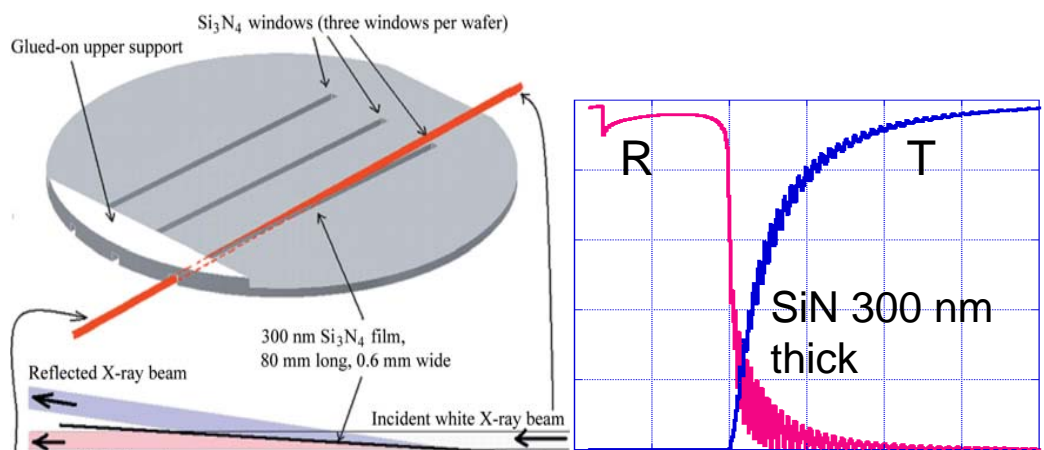


Transmition mirror: a high-pass energy filter

Silicon nitride transmission X-ray mirrors

Cornaby and D. H. Bilderback

J. Synchrotron Rad. 15, 371-373
(2008).

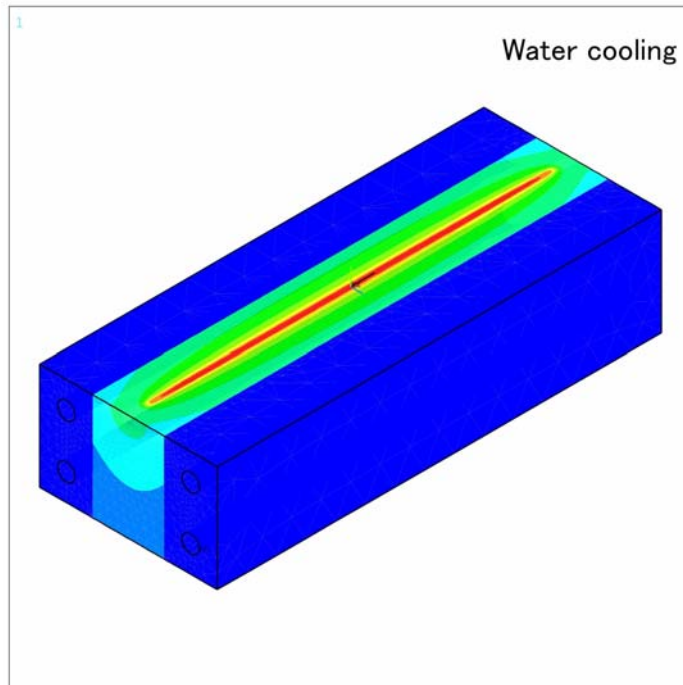


Heat load on and cooling of a mirror

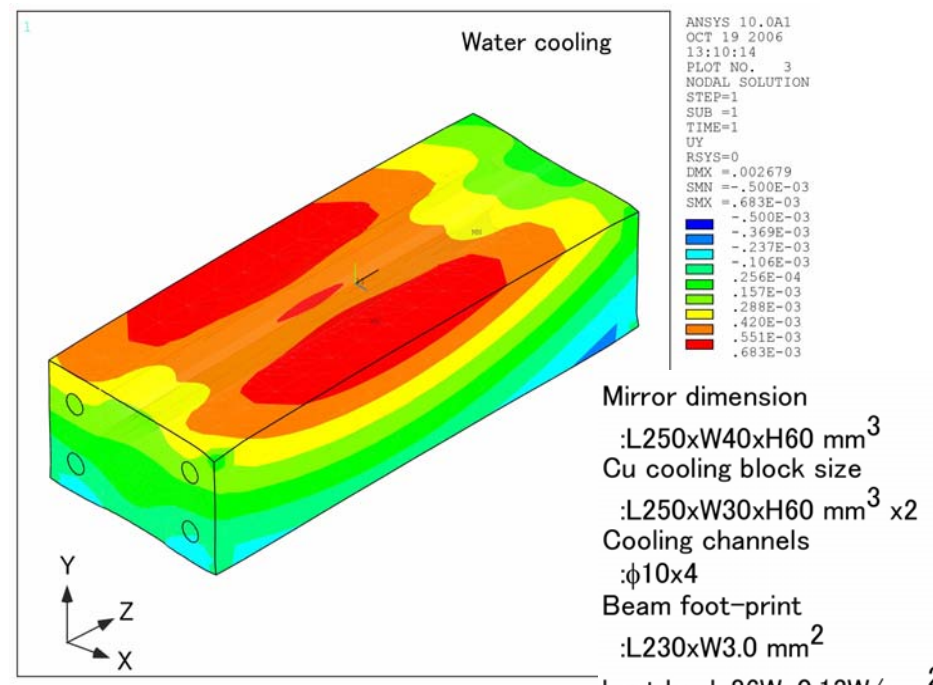
Heat load: 86 W, 0.13W/mm²

Glancing angle: 1.5° T_{water}=25°C

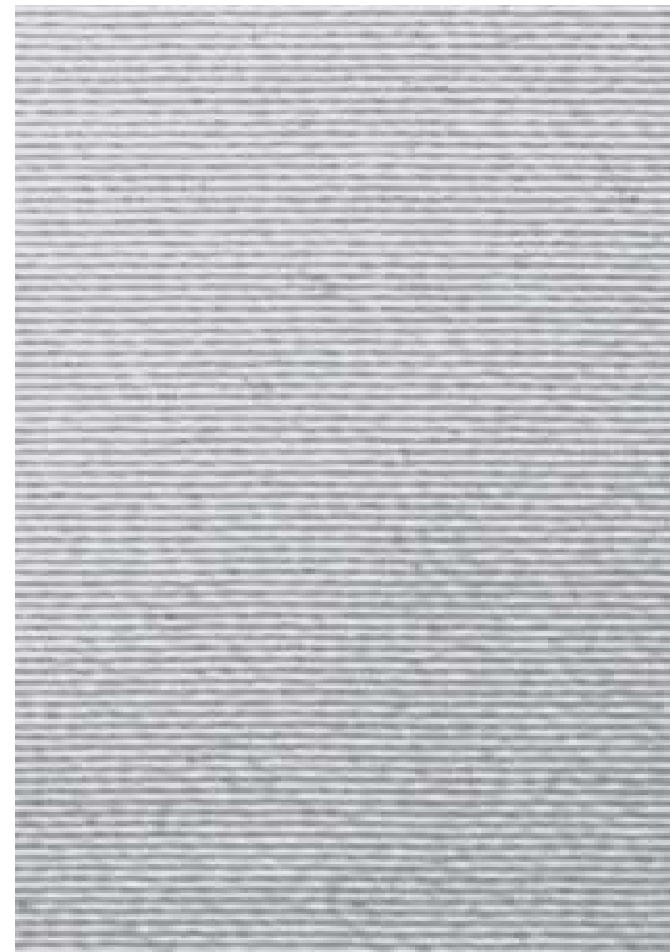
temperature



deformation



Multilayers



X-ray multilayer reflectivity

Recursive calculation of Fresnel coefficients and propagation

- Parratt formalism (widely used in x-ray optics) [8]

Principle

- Start at semi-infinite substrate surface (no reflection from back side)
- Recursive construction of amplitudes and phases from layer to layer

$$r_{n-1,n} = a_{n-1}^4 \cdot \left[\frac{r_{n,n+1} + f_{n-1,n}}{r_{n,n+1} f_{n-1,n} + 1} \right]$$

$f_{n-1,n}$: Fresnel coefficients

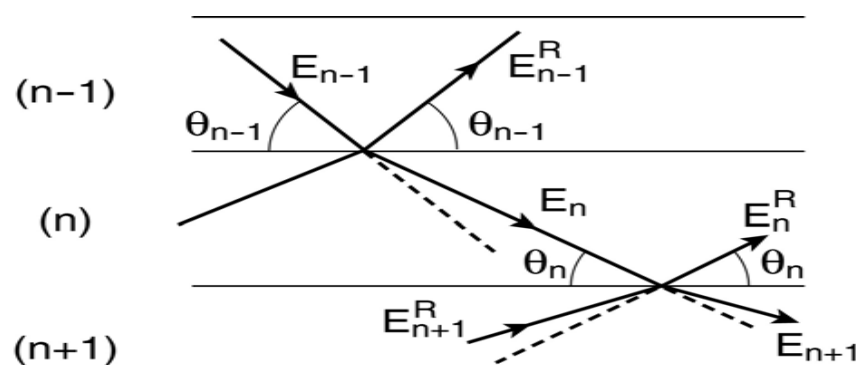
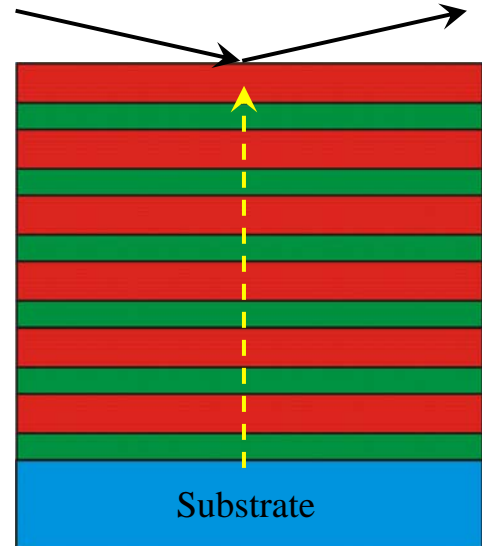
E_n : Electric field at centre of layer n

t_n : Thickness of layer n

$$r_{n,n+1} = a_n^2 \frac{E_n^R}{E_n}$$

$$a_n = e^{-i\frac{\pi}{\lambda}t_n\sqrt{n_n^2 - n_0^2}\cos^2\theta}$$

$$\rightarrow R = |r_{0,1}|^2$$



X-ray multilayer reflectivity

Numerical calculations

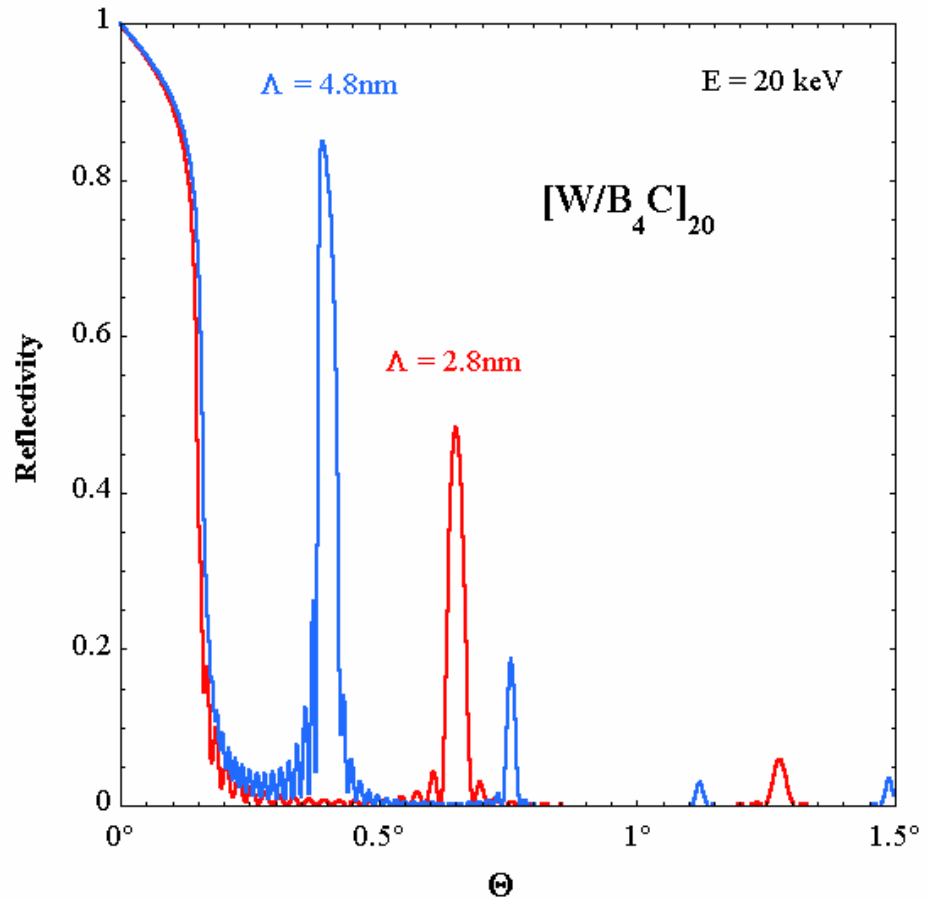
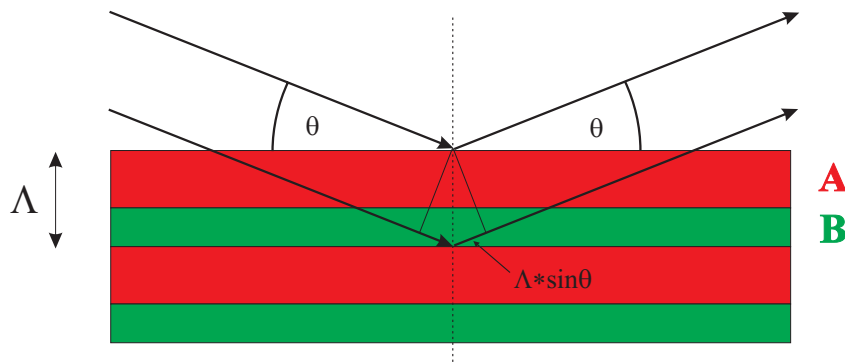
Main features

- Bragg peaks and fringes due to interference
- Positions depend on E and Λ
- Intensities depend on $\Delta \rho$, N, σ ...

Corrected Bragg equation

$$m \cdot \lambda = 2 \cdot \Lambda \cdot \sqrt{n_2^2 - n_1^2 \cos^2 \theta}$$

For $\theta \gg \theta_c \rightarrow m \cdot \lambda \approx 2 \cdot \Lambda \cdot \sin \theta$



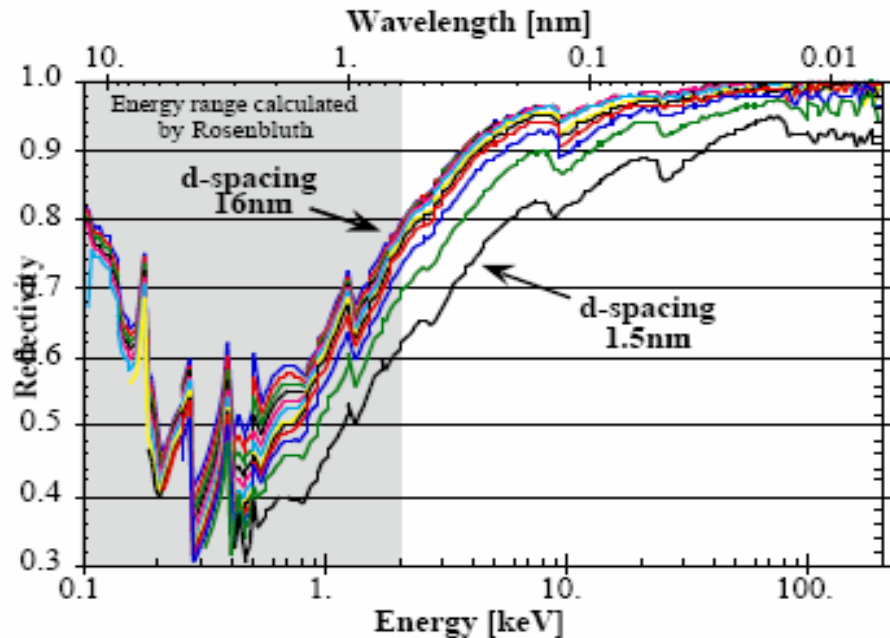
X-ray multilayer design

Materials choice – Basic rules:

1. Select low-Z spacer material with lowest absorption (β_{spacer})
2. Select high-Z absorber material with highest reflectivity with spacer ($\delta_{\text{abs}} - \delta_{\text{spacer}}$)
3. In case of multiple choices select high-Z material with lowest absorption (β_{abs})
4. Make sure that both materials can form stable and sharp interfaces (lower d-spacing limit)

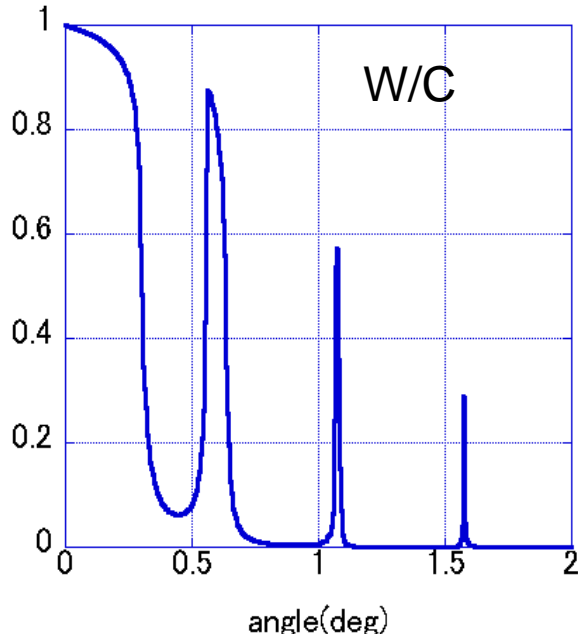
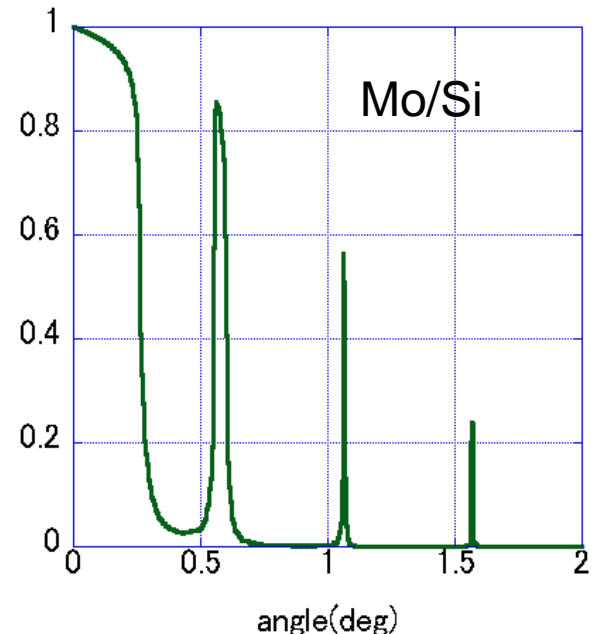
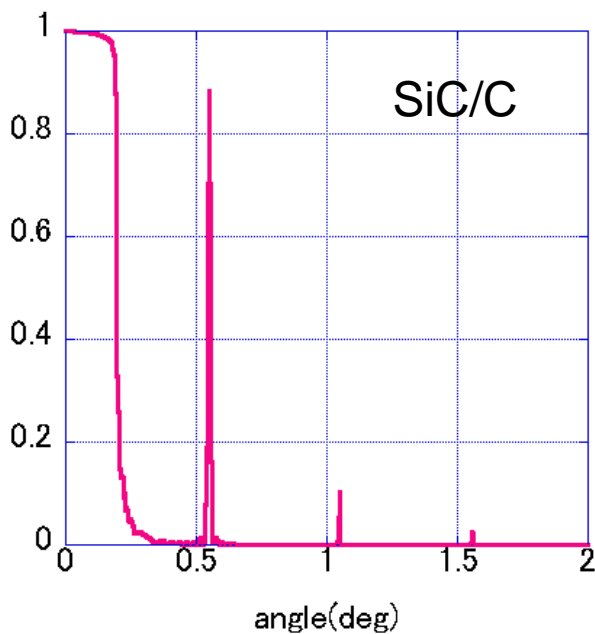
Computational search algorithms

- Soft X-rays: A.E. Rosenbluth (1988)
- Hard X-rays: K. Vestli (1995)



[9] K. Vestli, E. Ziegler, Rev. Sci. Instr. 67, 3356 (1996)

	Atomic number	Density (g/cm3)
C	6	2.26
Si	14	2.33
SiC	-	3.2
Mo	42	10.22
W	74	19.35



X-ray multilayer design

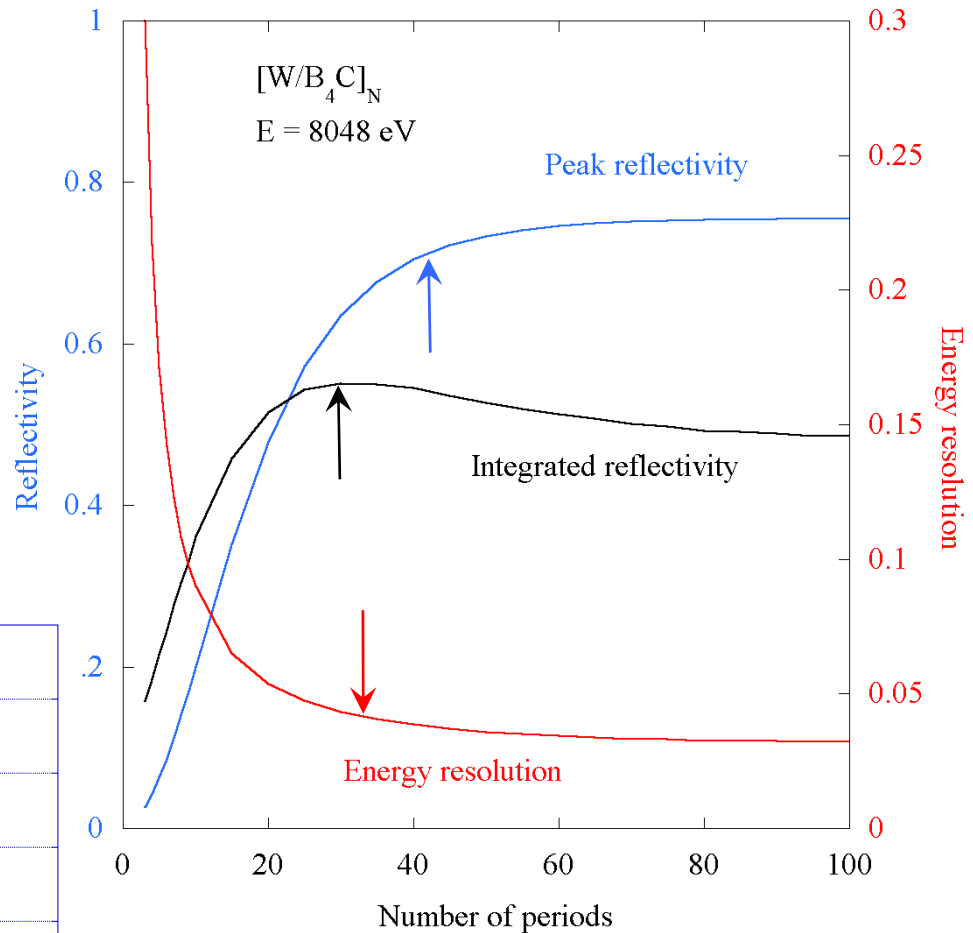
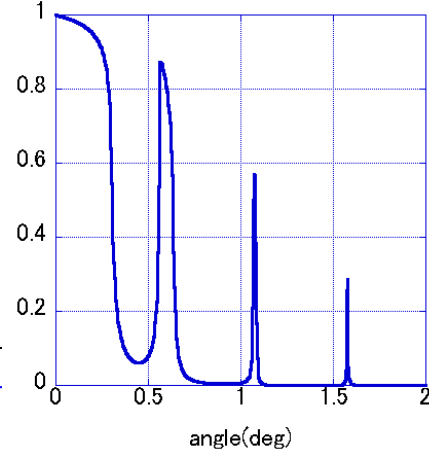
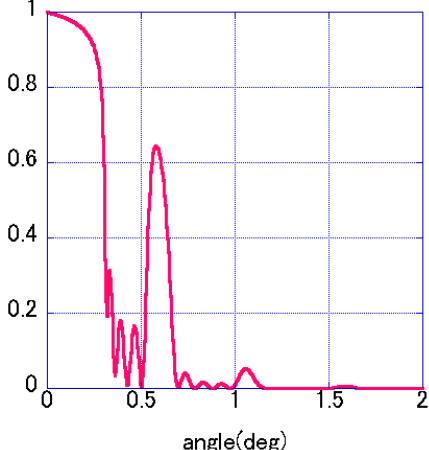
Period number N:

Peak versus integrated reflectivity:

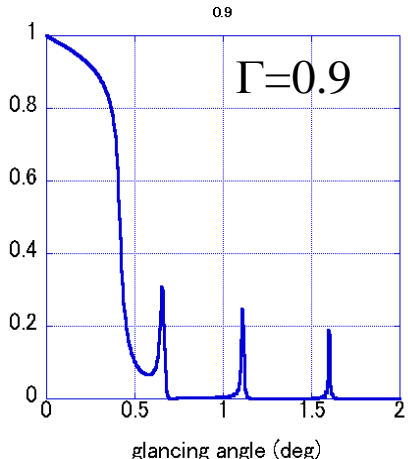
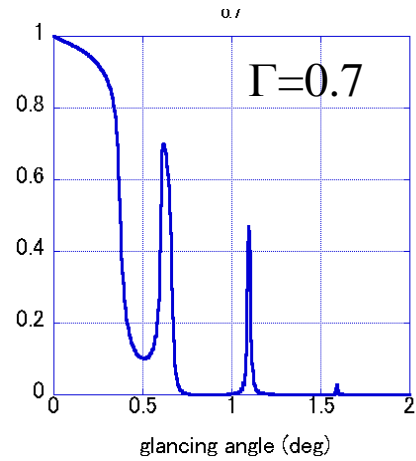
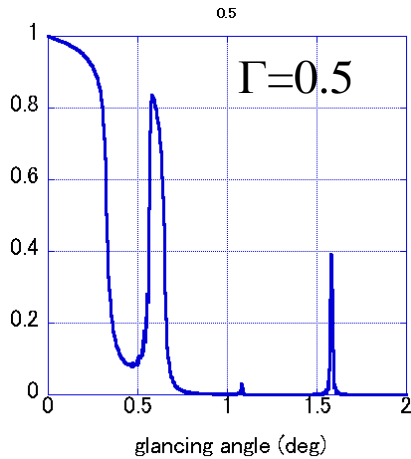
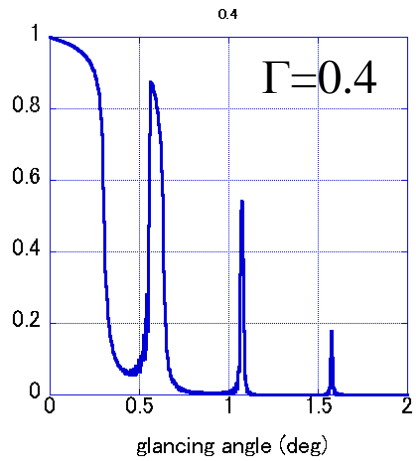
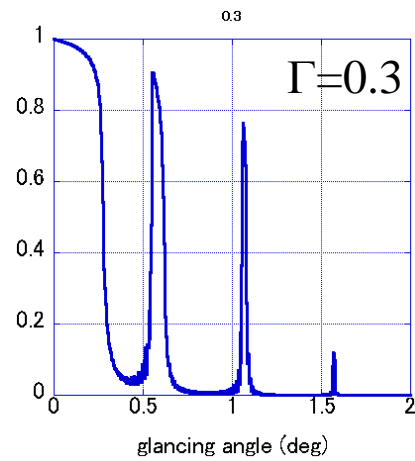
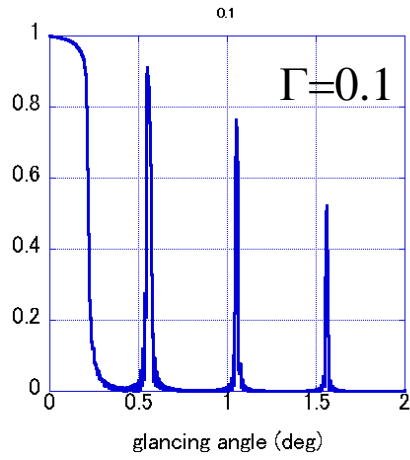
- R_{peak} increases with N up to extinction
- $\Delta E/E$ decreases $\sim 1/N$ in kinematical range
- R_{int} is maximum before extinction

High and low resolution MLs

Optimize N according to needs !

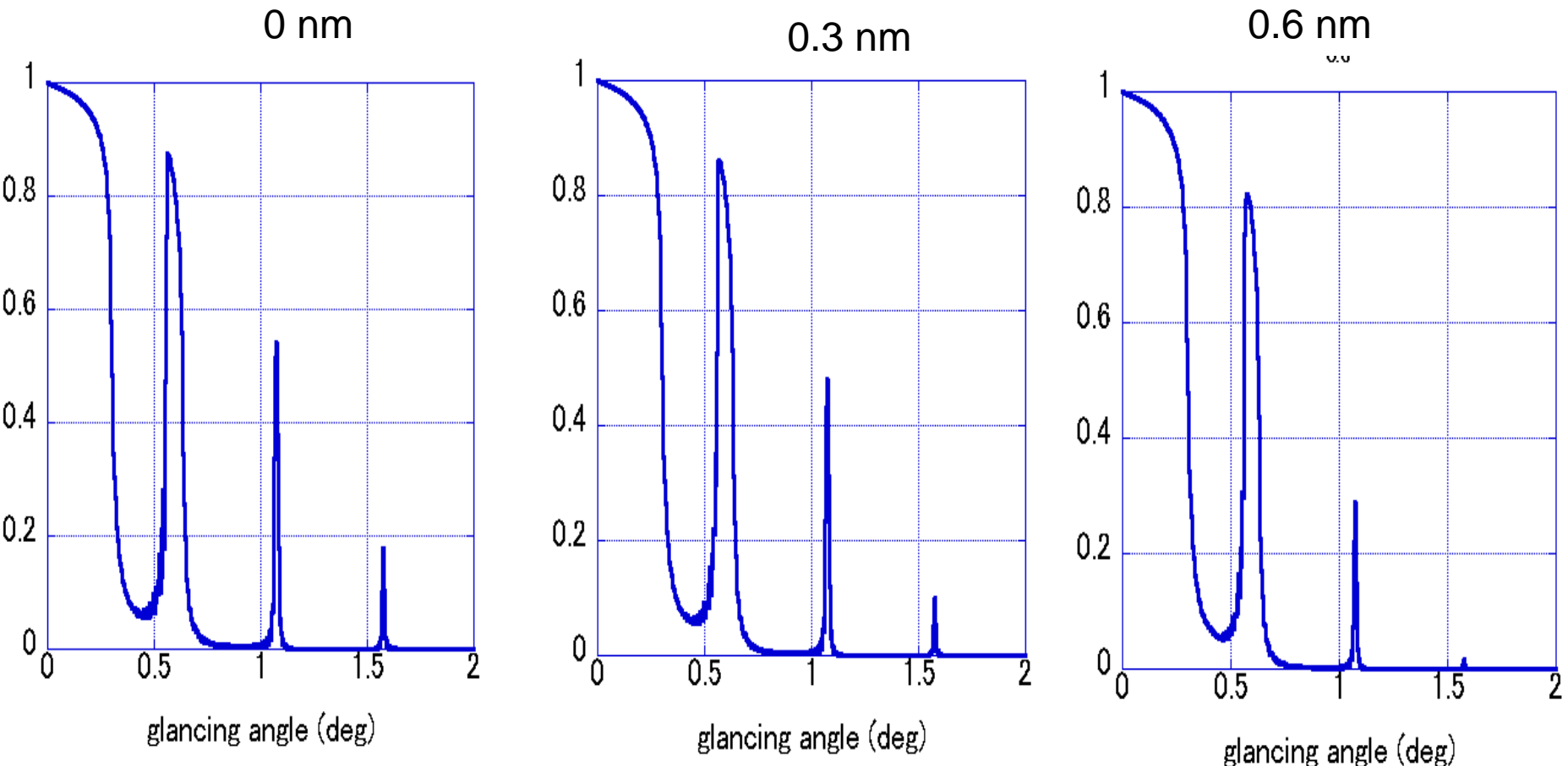


W/C multilayer $\Gamma=t_W/\Lambda$



Effect of interlayer diffusion

C/W $\Lambda=6.9$ nm $\Gamma=0.4$



X-ray multilayer fabrication

Deposition techniques	Vacuum	Particle energy	Deposition rate	Deposition area
Thermal evaporation	HV (UHV)	Low	Low	Small
E-beam evaporation	UHV	Low	Low	Small
Magnetron sputtering	HV (+Gas)	High	High	Large
DECR sputtering	HV (+Gas)	High	Low	Medium
Ion beam sputtering	UHV (+Gas)	Very high	High	Medium
Pulsed laser deposition	HV	Very high	High	Medium

- Characteristics may vary depending on equipment and application
- Magnetron sputtering most widely used for X-ray multilayer fabrication
- Vacuum and purity important for EUV and soft X-rays
- High particle energy favors very thin and uniform layers

X-ray multilayer fabrication

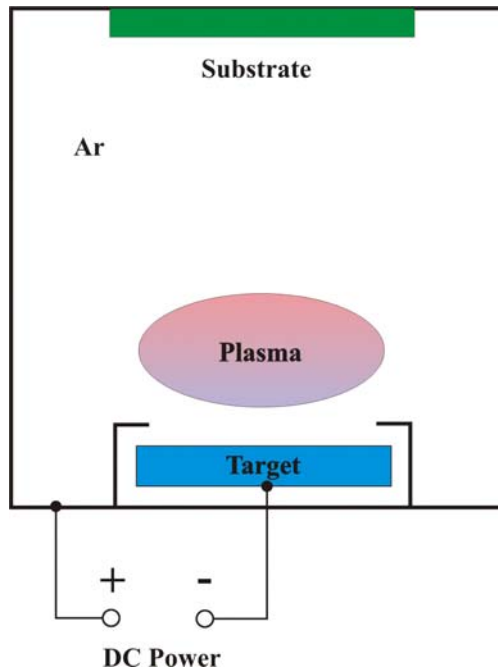
History

1923	Koeppe	Cd/Ag	electrolysis	unstable
1930	Deubner	Au/Ag	electrolysis	unstable
1935	Dumond	Au/Cu	thermal evaporation	1 week life time
1963	Dinklage	Me/Mg	thermal evaporation	stable
1972	Spiller	Au/MgF₂	thermal evaporation	UV MLs
1976	Haelbich	Me/C	thermal evaporation	XUV MLs
1978	Barbee	W/C	magnetron sputtering	X-ray MLs
1983	Gaponov	Me/C	pulsed laser deposition	X-ray/VUV MLs

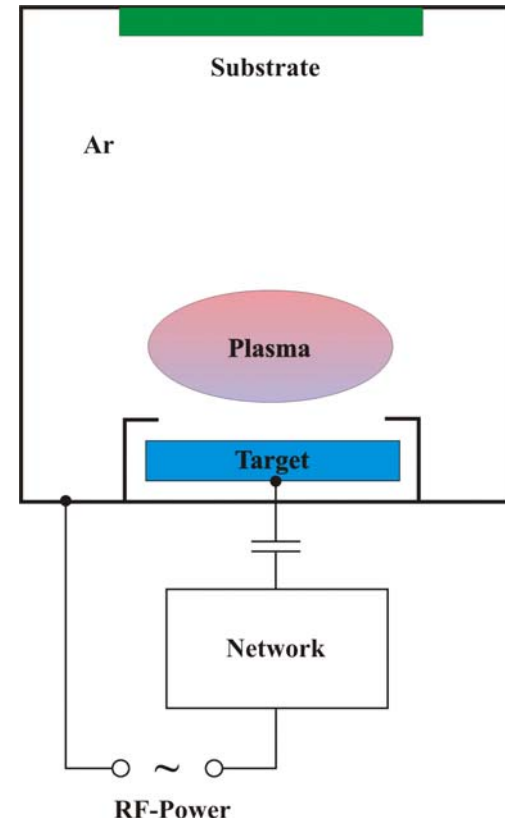
X-ray multilayer fabrication

Sputtering techniques

DC (conductors)



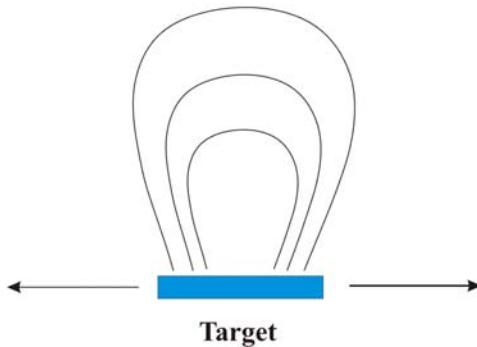
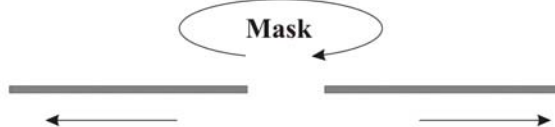
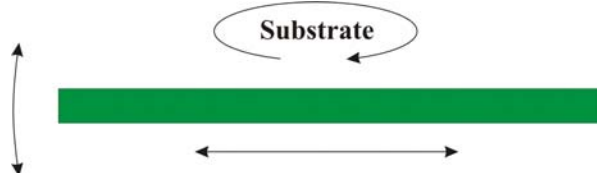
RF (insulators)



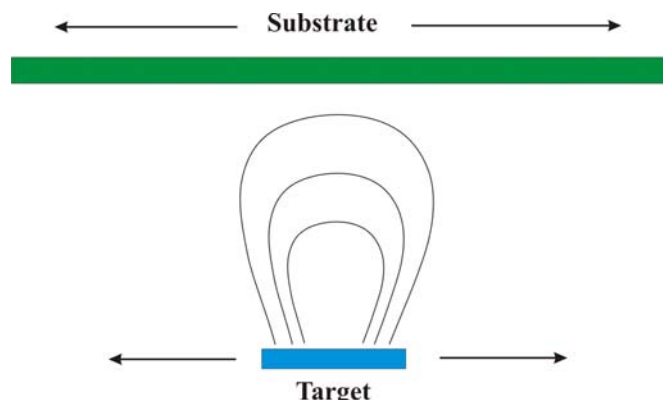
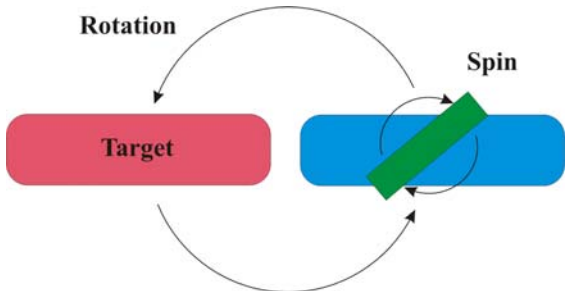
X-ray multilayer fabrication

Large area coatings (uniform, gradient)

- Relative motion source - substrate
- Masking techniques

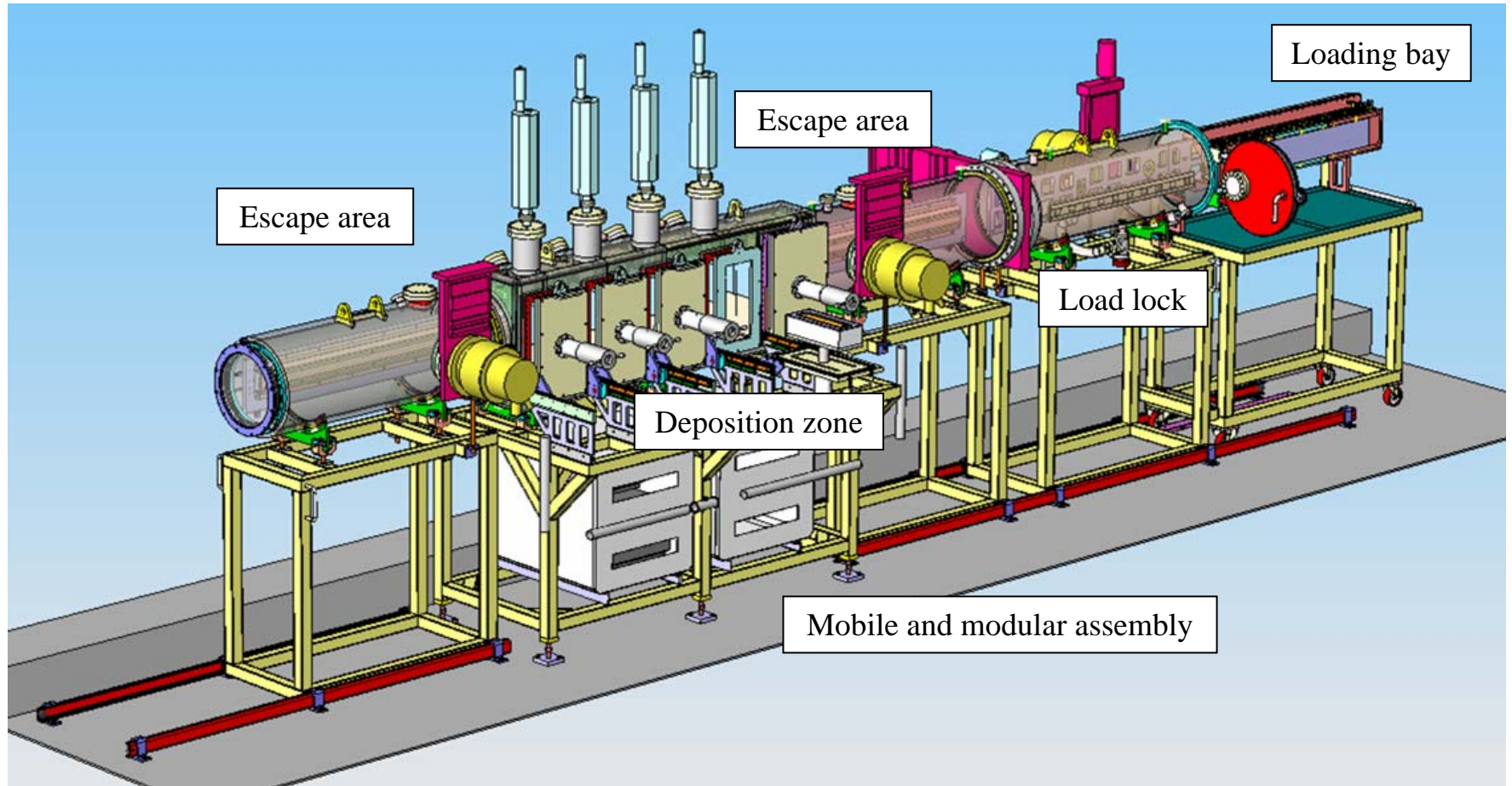


$$t(\vec{r}) = \int \varphi(\vec{r}, \vec{r}') \frac{d\vec{r}'}{v(\vec{r}')}$$



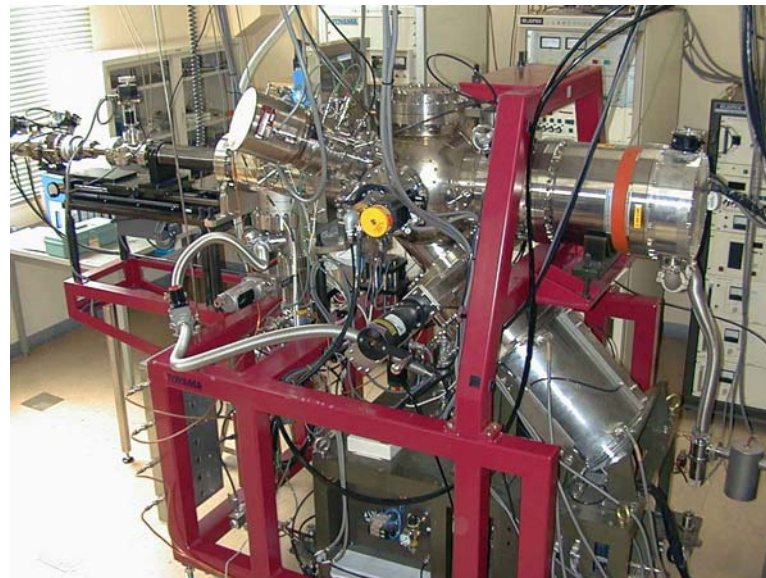
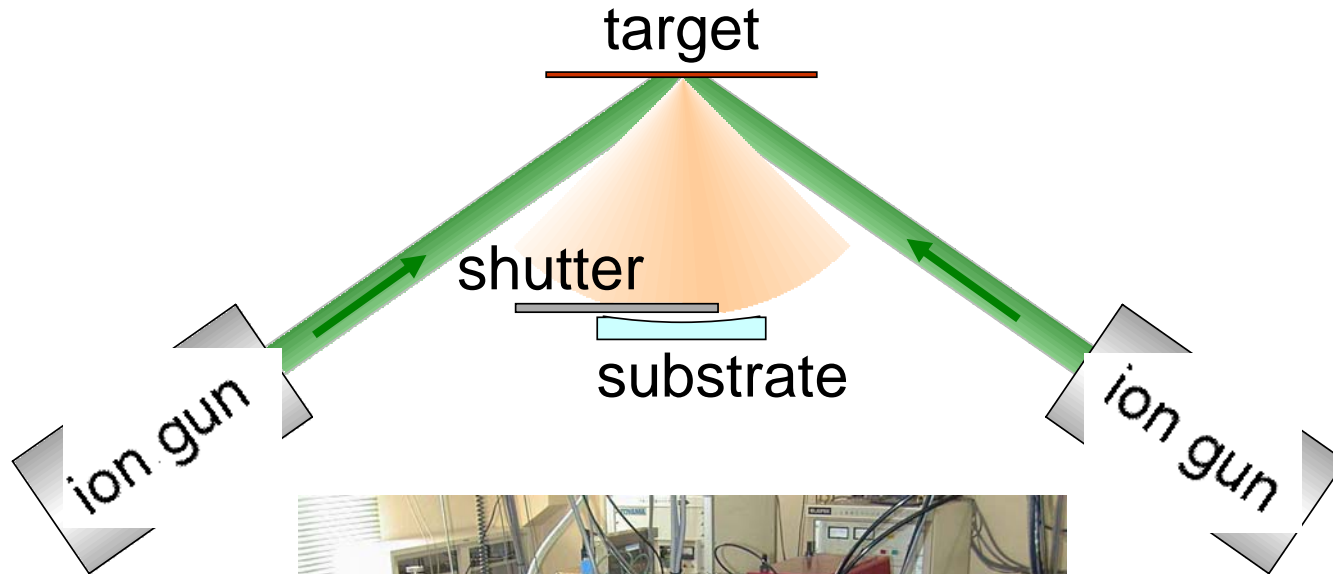
X-ray multilayer fabrication

ESRF magnetron sputter deposition system



X-ray multilayer fabrication

Sputtering techniques (**Ion beam** sputtering at Tohoku Univ.)



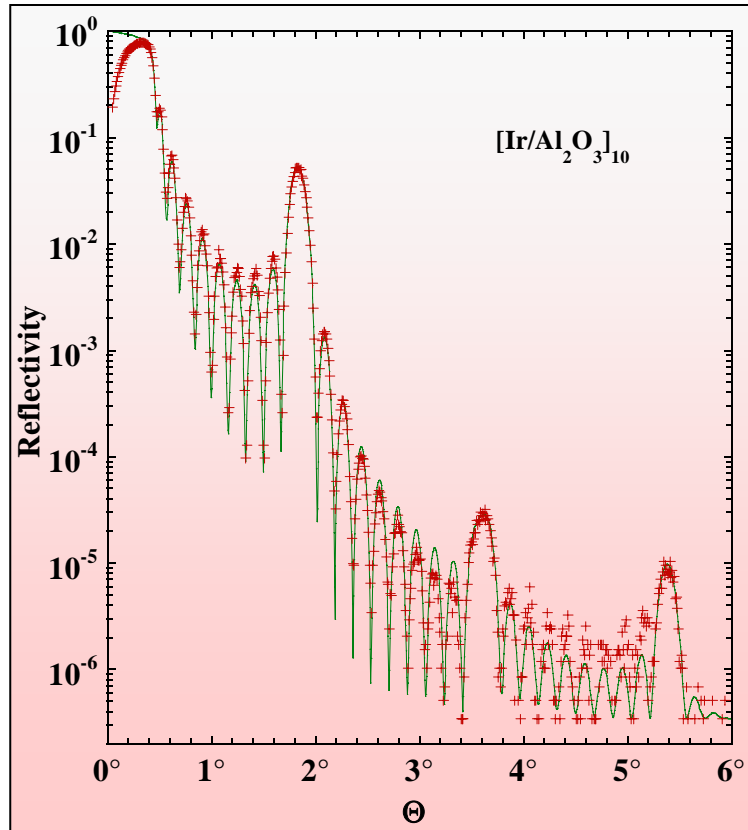
TEM
Mo/Si
 $D = 6.9 \text{ nm}$
 $\lambda = 13.5 \text{ nm}$
 $\phi = 5^\circ$

TEM
Cr/Sc
 $D = 1.77 \text{ nm}$
 $\lambda = 3.1 \text{ nm}$
 $\phi = 27.5^\circ$

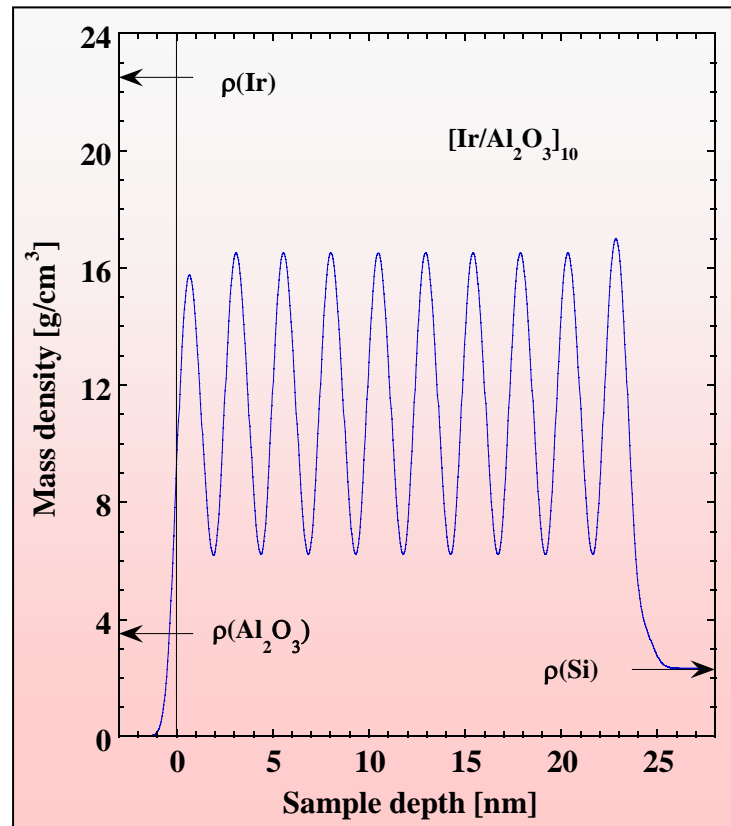
X-ray multilayer characterization

X-ray reflectivity

Simulation of x-ray reflectivity



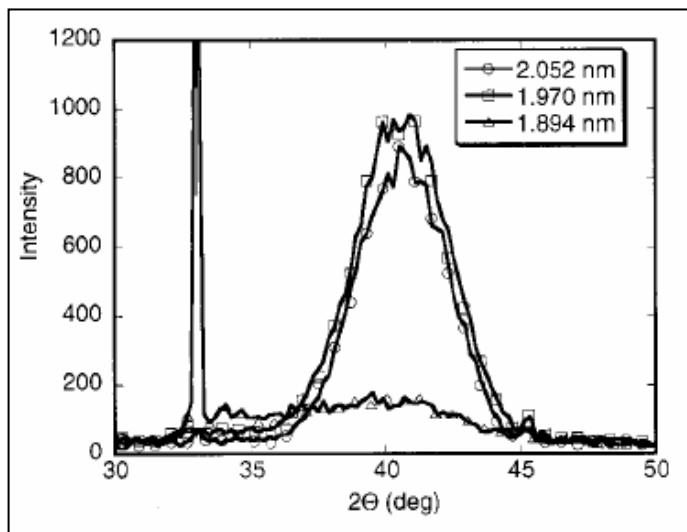
Vertical density profile



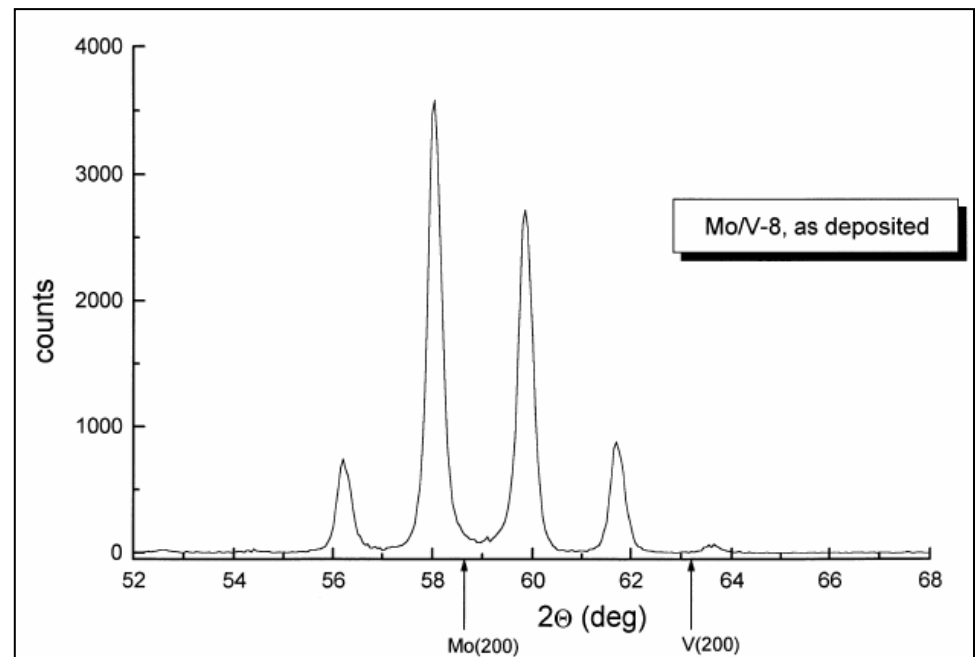
X-ray multilayer characterization

X-ray scattering

- Access to atomic structure
- Phase transitions
- Coherence lengths
- Superlattice formation



[16] S. Bajit et al, J. Appl. Phys. 90, 1017 (2001)



[17] D.L Beke et al, Vacuum 50, 373 (1998)

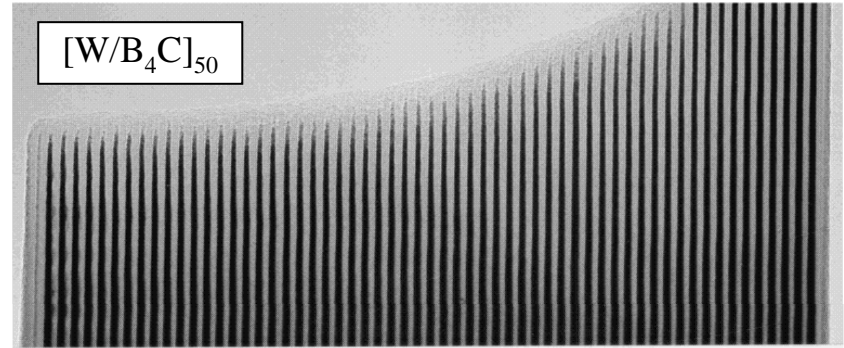
X-ray multilayer characterization

Transmission electron microscopy (TEM)

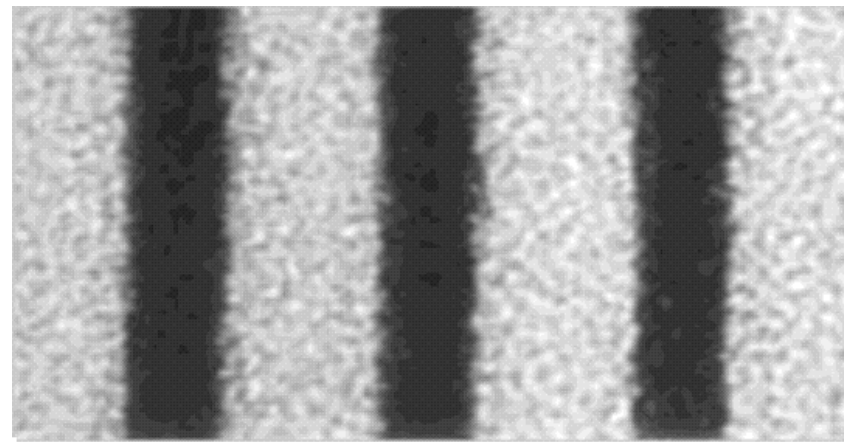
- Fabrication errors
- Roughness evolution
- Crystallinity
- Interface diffusion



Complementary to x-ray measurements !



100 nm



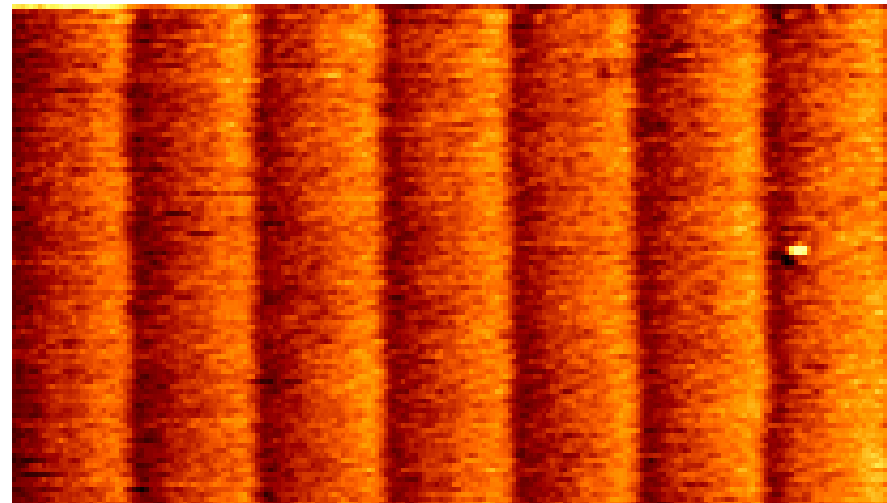
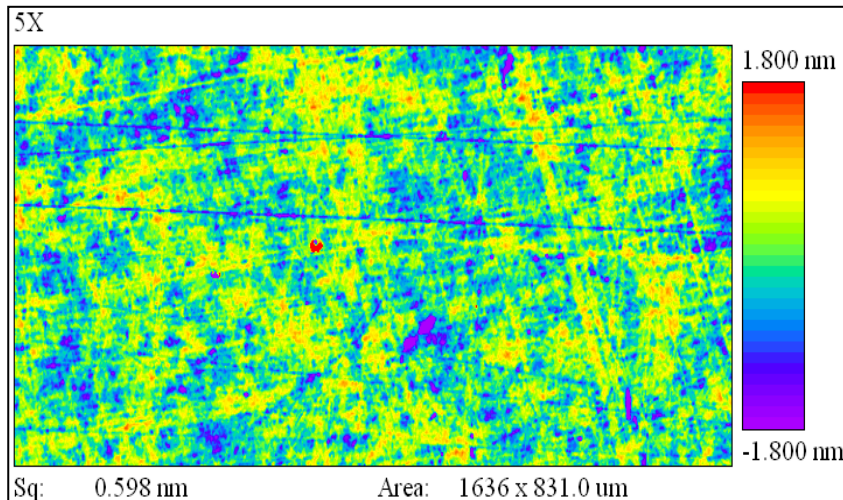
R. Scholz, MPI Halle, Germany

X-ray multilayer/mirror characterization

Surface metrology

- Atomic Force Microscopy (AFM)
- Interferometry
- Long Trace Profiler (LTP)
- From nm to m scale
- No depth information !

A. Rommevaux, ESRF Optics Group



X-ray multilayer design

Aperiodic design:

Goal: ML with particular reflectivity profile

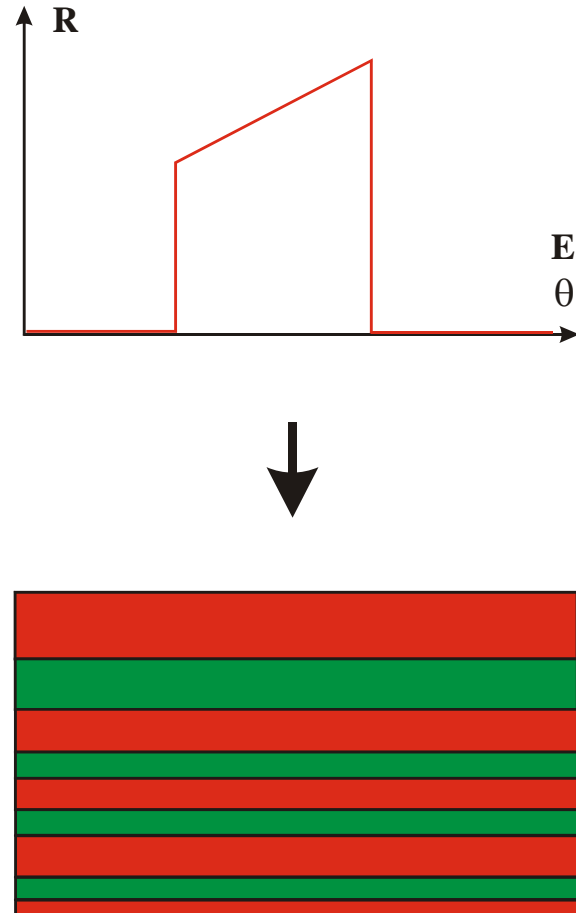
- $R = R(\theta)$ for $E = \text{const}$
- $R = R(E)$ for $\theta = \text{const}$

Find vertical composition profile

Method:

- Derive analytical expression for reflectivity
- Do inversion to obtain 1st estimate for layer sequence
- Apply fit algorithm to optimize the structure

[12] I.V. Kozhevnikov et al, Nucl. Instr. And Meth. A 460, 424 (2001)



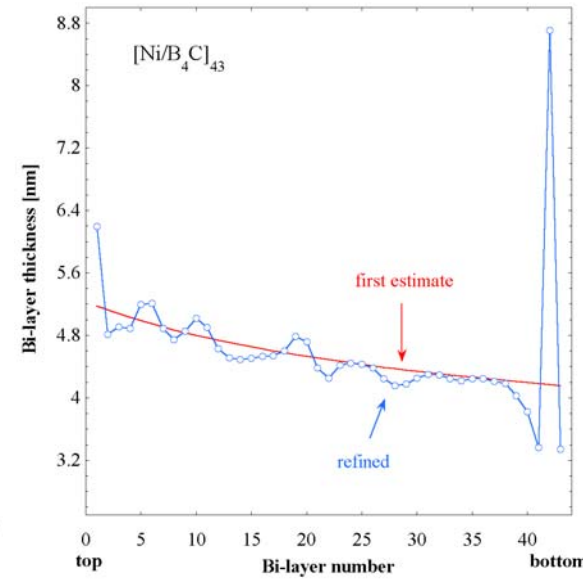
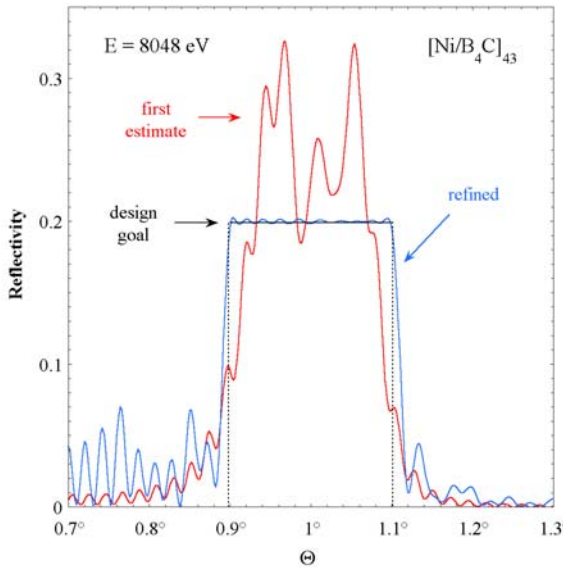
X-ray multilayer design

Example:

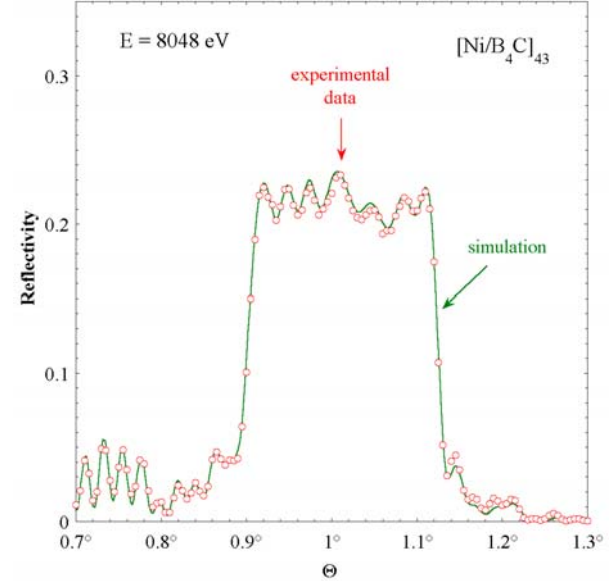
- Ni/B₄C structure
- R(θ) = const over 20% bandwidth

[13] Ch. Morawe et al, Nucl. Instr. And Meth. A 493, 189 (2002)

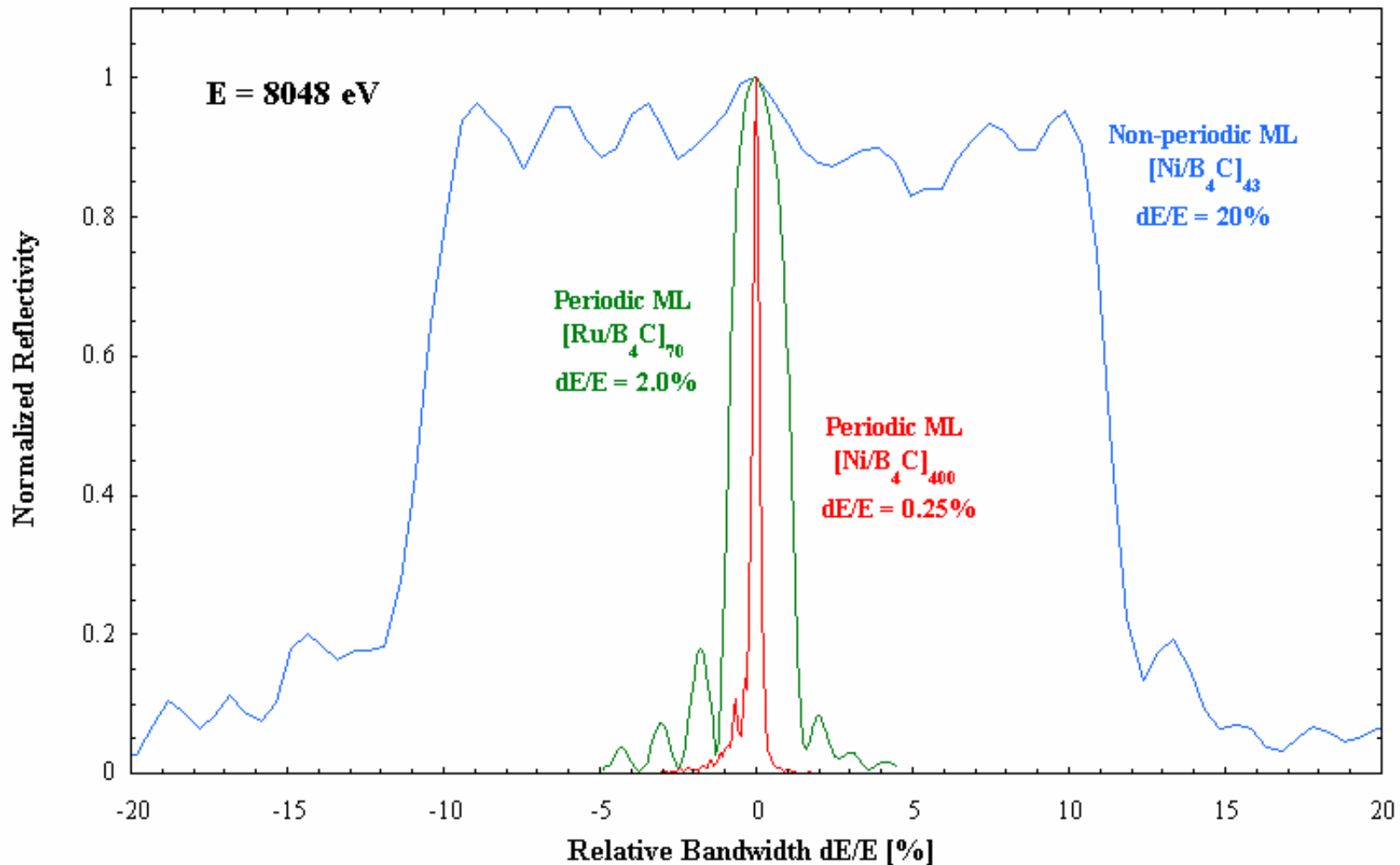
Theoretical design



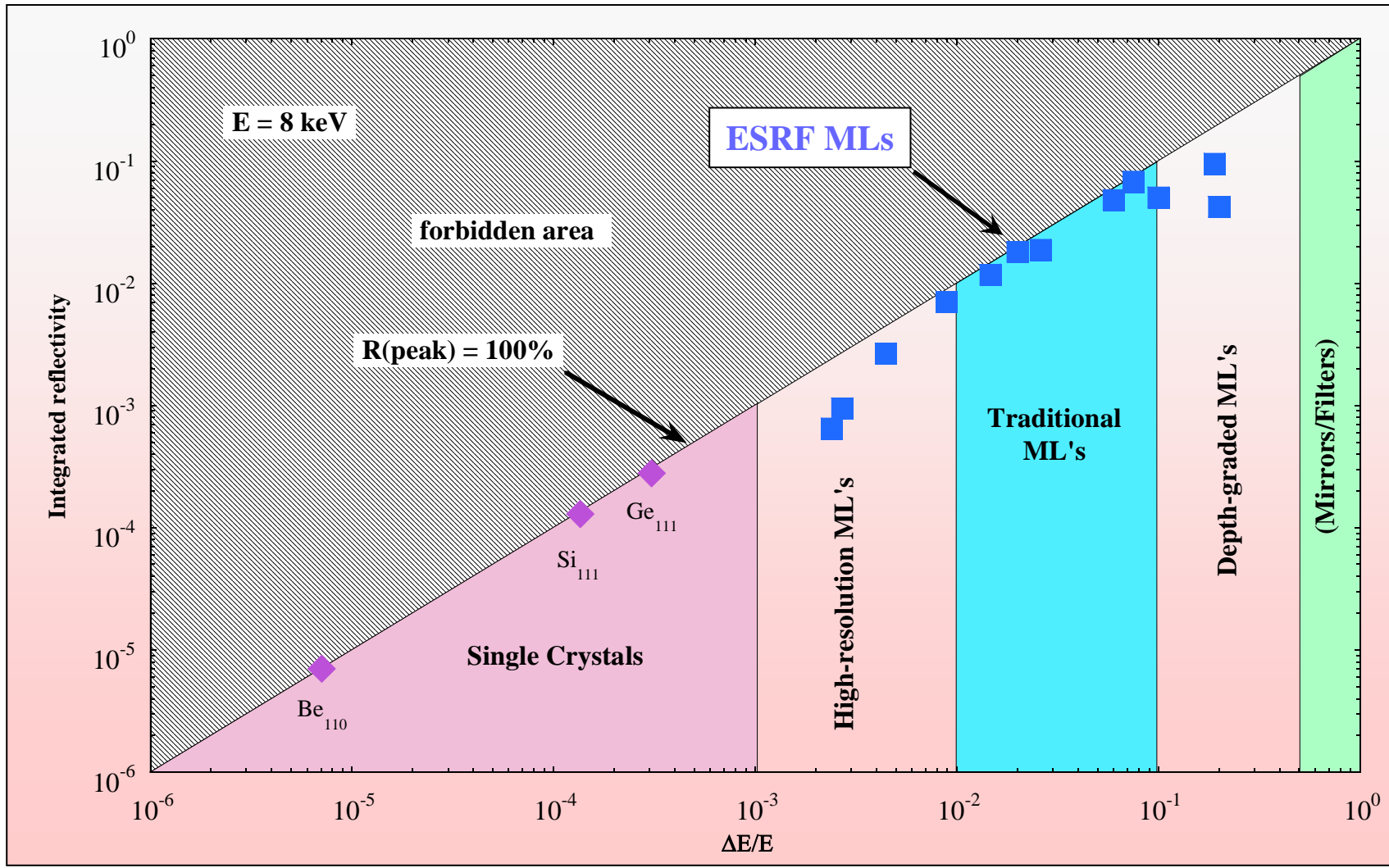
Experimental result



Energy resolution of multilayers



Reflecting X-ray optics – Overview



Laterally graded multilayers

Surface curvature and beam divergence define lateral gradient $d\Lambda / dx$

Shape

Parabolic

Elliptic

Flat

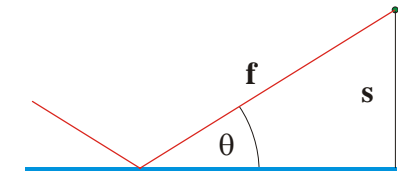
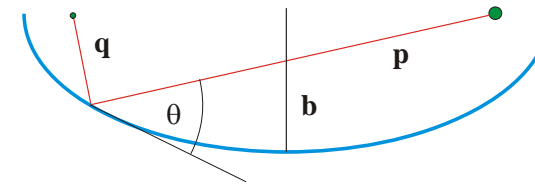
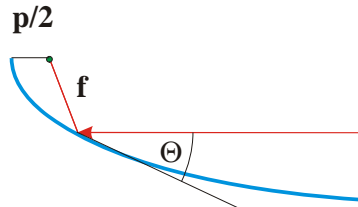
Angle θ

$$\sin \theta = \sqrt{\frac{p}{2f}}$$

$$\sin \theta = \frac{b}{\sqrt{pq}}$$

$$\sin \theta = \frac{s}{f}$$

Geometry

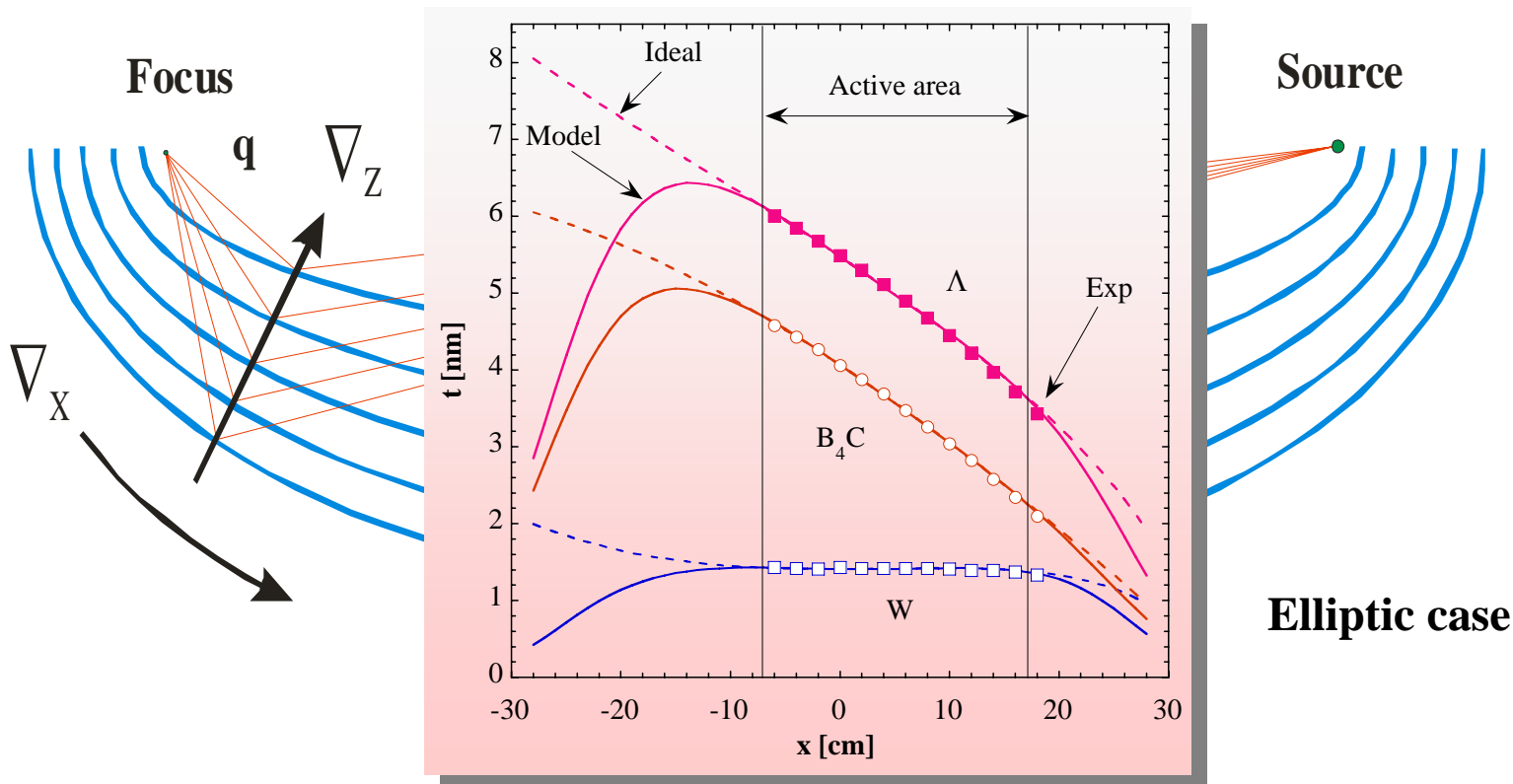


**d-spacing including refraction correction
(modified Bragg equation)**

$$\Lambda = \frac{\lambda \cdot m}{2\sqrt{n^2 - \cos^2 \theta}}$$

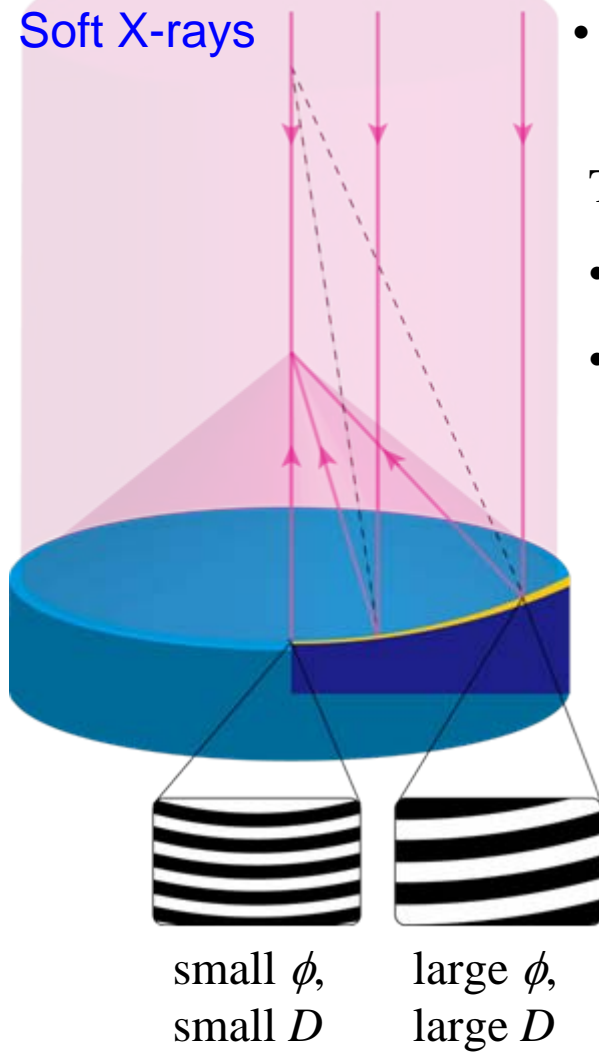
Laterally graded multilayers

- Divergent beam, focusing applications with curved substrates
- Incidence angle variation → laterally graded multilayers
- Additional depth gradient negligible ($< 10^{-5}$)



laterally graded multilayers

Soft X-rays



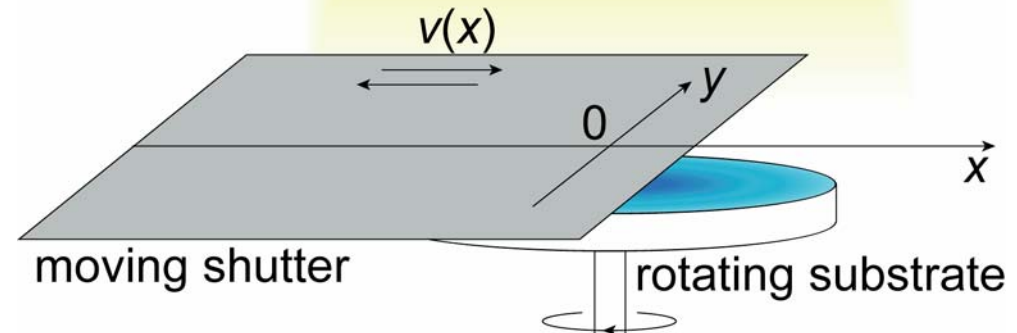
- Divergent beam, focusing applications with curved substrates
- Angle of incidence variation → laterally graded multilayers

Thickness control by

- Relative motion of source - substrate (in magnetron sputtering)
- Moving shutter (for a large gradient)

Ion beam sputtering

sputtered material



Double graded multilayers

Energy dispersion:

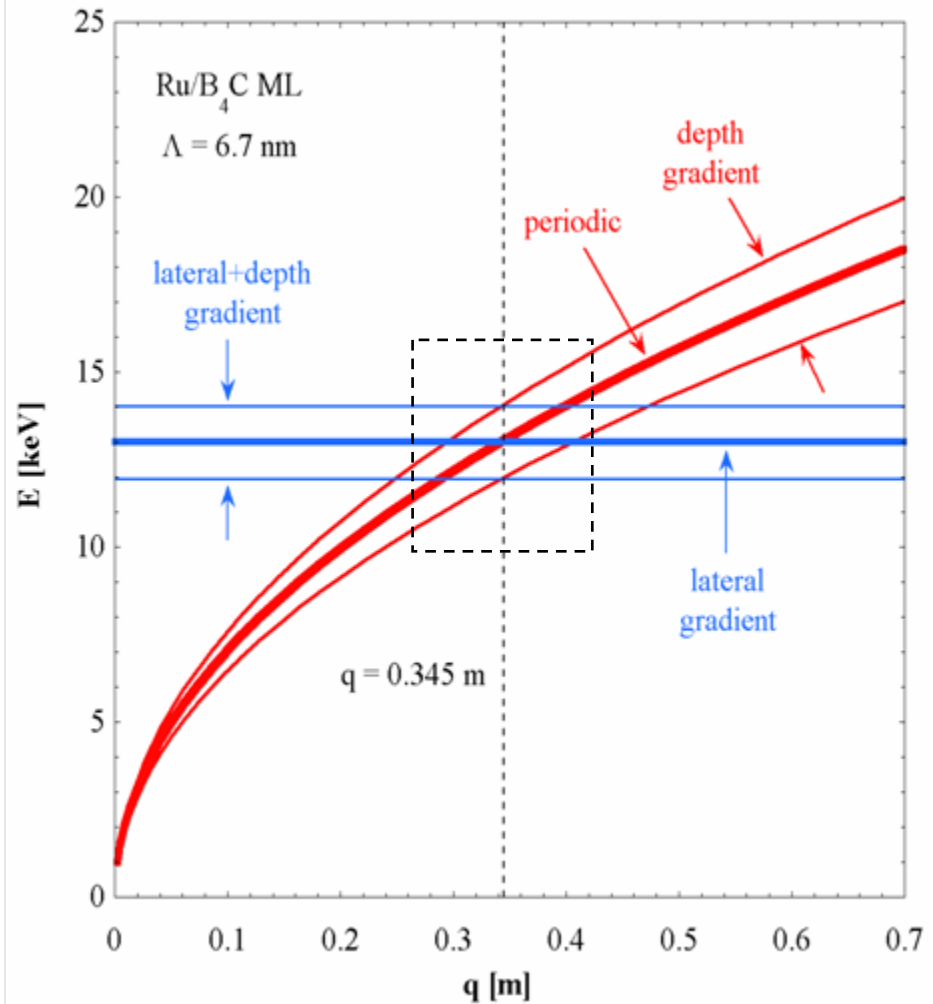
Bragg equation: $E(\theta) = \frac{h \cdot c}{2\Lambda \sqrt{n^2(E) - \cos^2 \theta}}$

Elliptic mirror: $\sin^2 \theta = \frac{b^2}{p \cdot q} \quad p + q = 2 \cdot a$



$$E(q) = \frac{h \cdot c}{2\Lambda \sqrt{n^2(E) - 1 + \frac{b^2}{(2a-q)q}}}$$

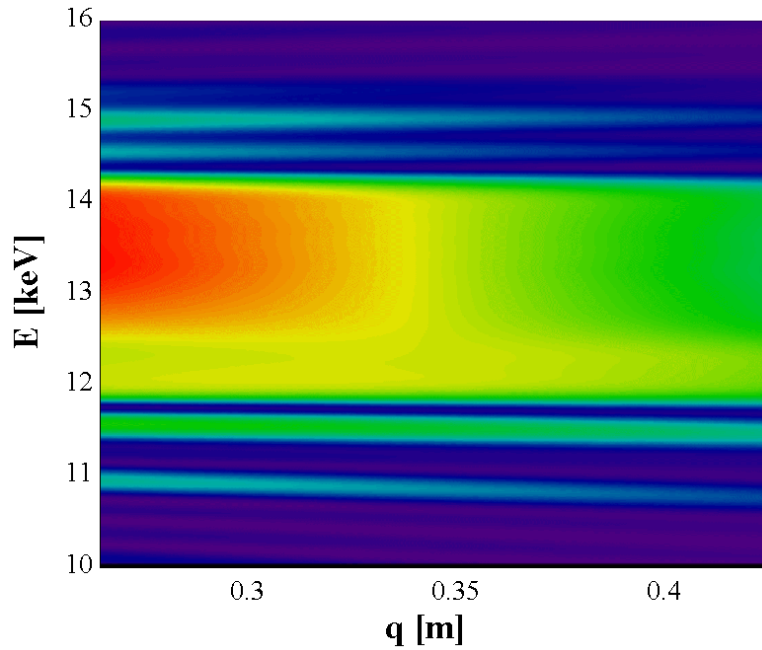
Dispersion “along ML mirror”



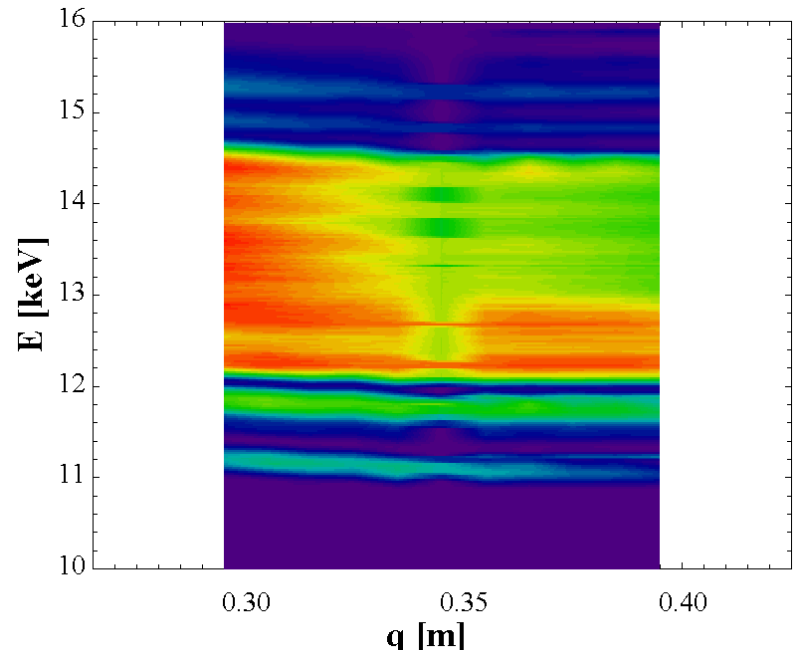
Double graded multilayers

Intensity profiles: (Kirkpatrick-Baez multilayer optics on ESRF BM05)

Theory



Experiment

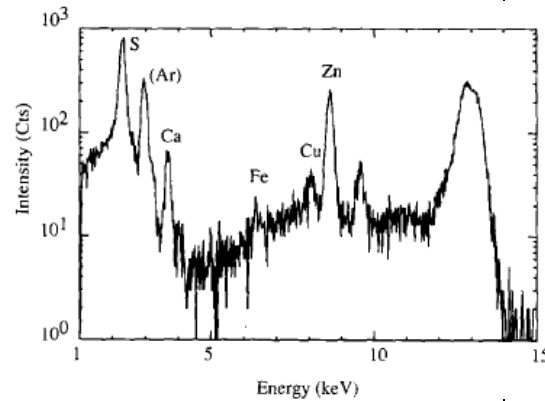
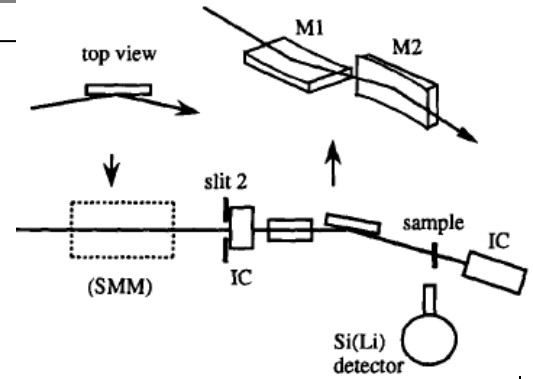
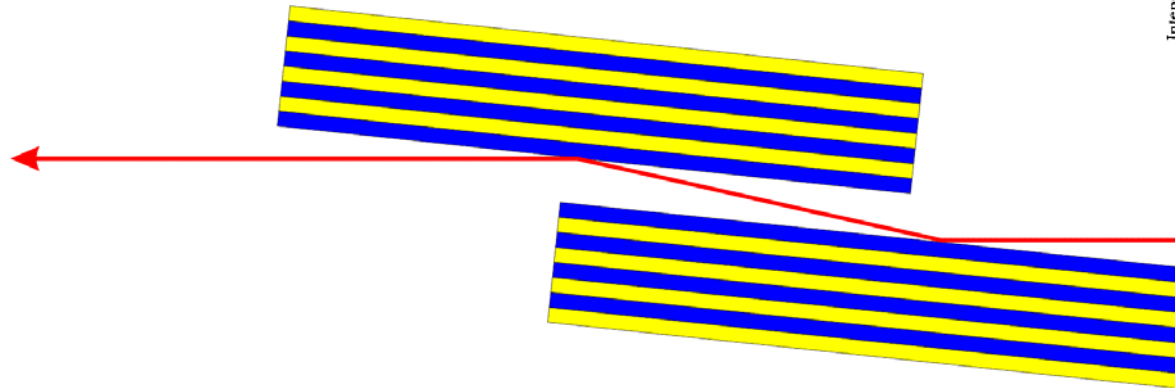


[14] Ch. Morawe, Ch. Borel, E. Ziegler, J-Ch. Peffen, Proc SPIE 5537, 115 (2004)

Applications

Synchrotron optics: Multilayer high flux monochromators

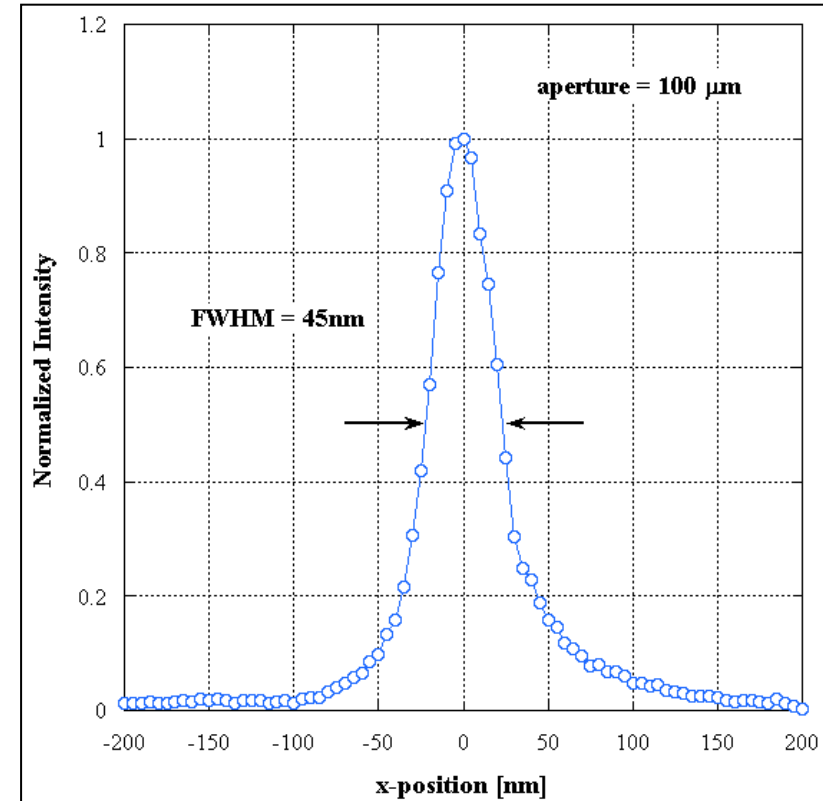
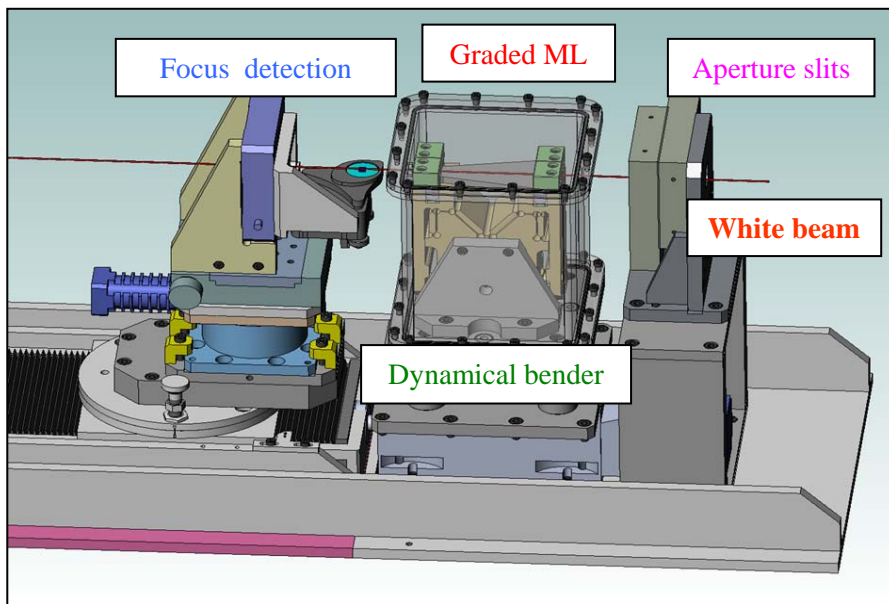
- Two bounce optics
- 100x larger bandwidth compared with Si(111)
- Harmonics suppression due to refraction and filling factor
- **Radiation and heat load issues !**



Applications

ESRF focusing experiment

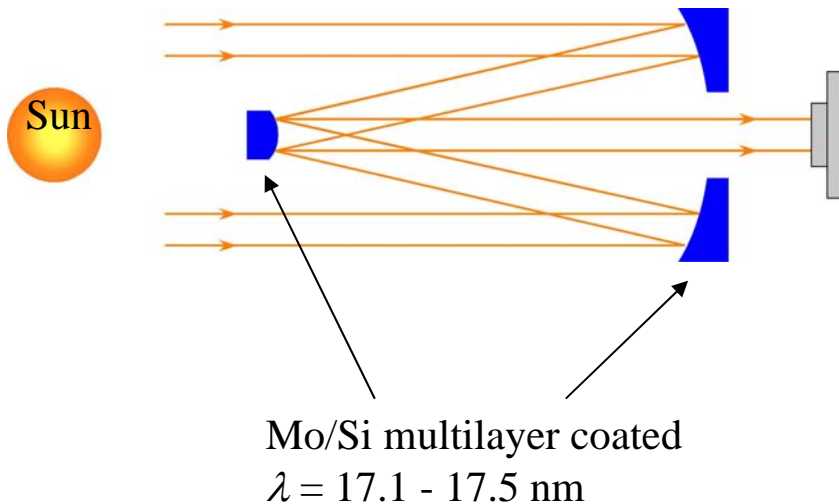
- Full undulator spectrum
- Vertical line focus
- Dynamical bender
- Raw data **45 nm FWHM @ 100 μ m aperture**



[24] Ch. Morawe et al, Proc. SPIE 6317 (2006)

Multilayer application –Telescope–

Rocket launched Cassegrain telescope

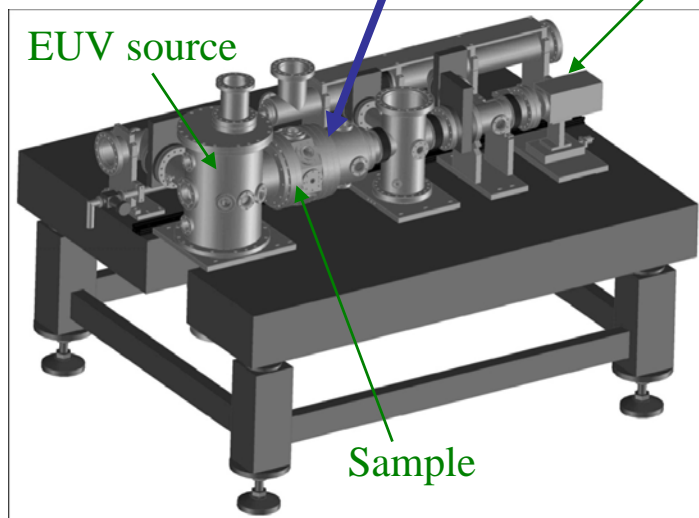
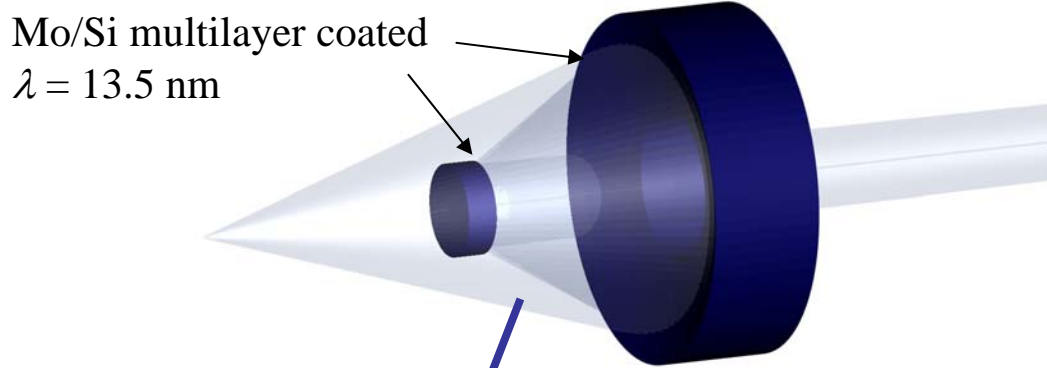


David Attwood

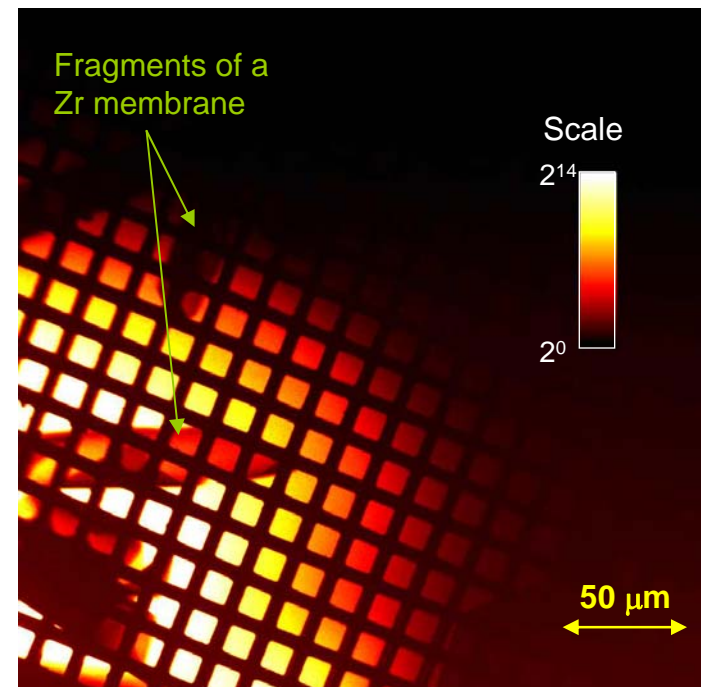
Soft X-rays and extreme ultraviolet radiation – Principles and Applications –
(Cambridge University Press 1999).

Multilayer application –Microscope–

Schwarzschild objective of a laboratory microscope

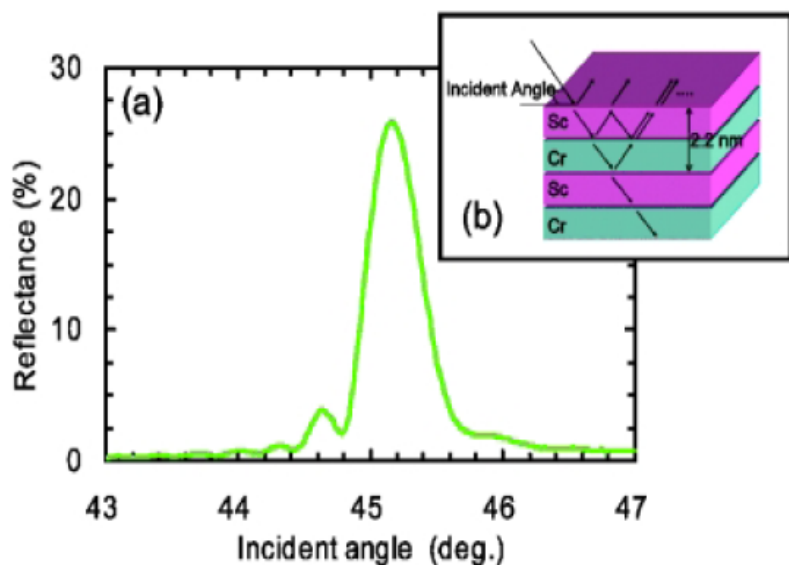


Transmission image of
#1500 Cu mesh (50 \times)



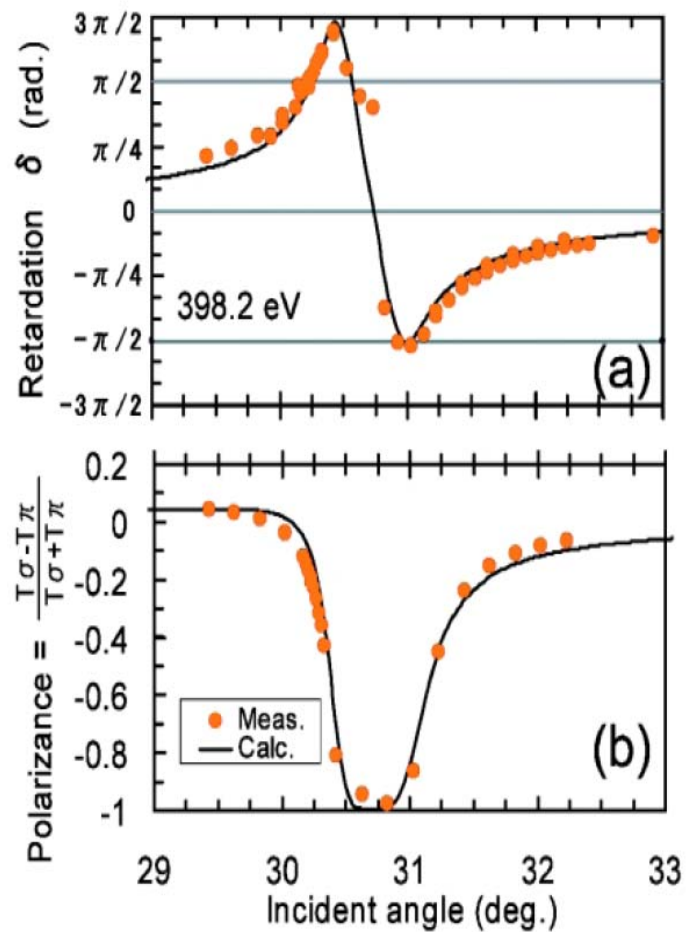
Yamamoto and Yanagihara group, Tohoku Univ.

Multilayer phase plate



Polarization characteristics of a transmitting Sc/Cr phase shifter.

M. Suzuki and Hirono, 放射光 Nov. 2006,
Vo.19 No6, pp.444-453

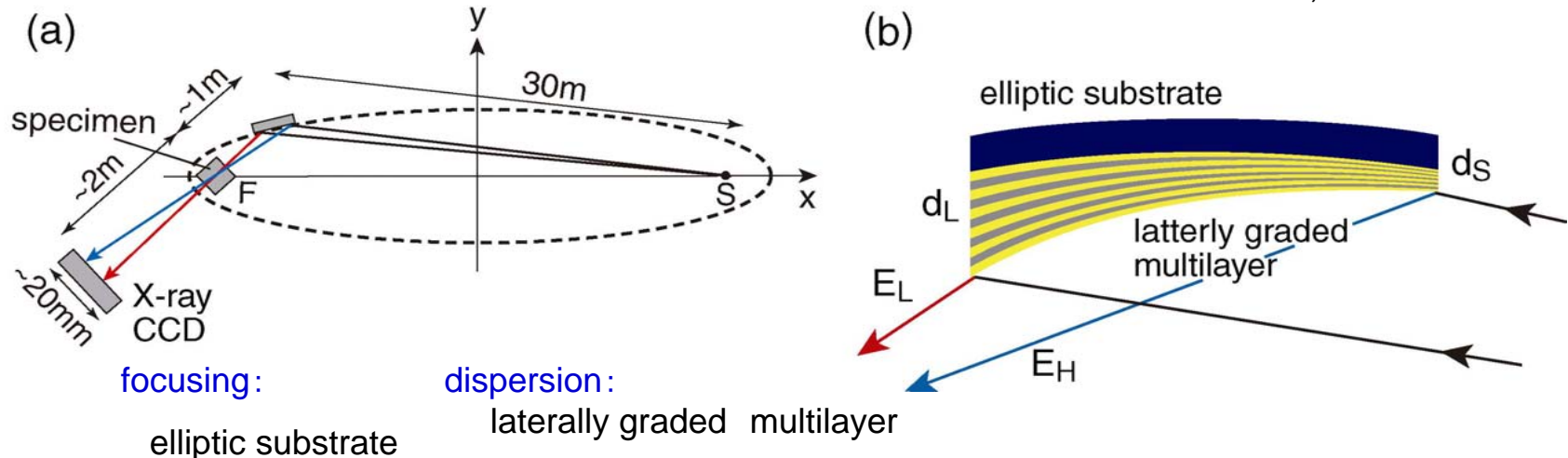


Reflectance of a $[\text{Sc}(2.2 \text{ nm})/\text{Cr}(2.2 \text{ nm})]_{200}$ multilayer, which works as a reflecting polarizer.

Application

Simultaneous measurement of X-ray reflectivity curve Laterally d-graded multilayer on an elliptic surface

T. Matsushita et. al., 2008



Other issues

- Brewster's angle, p-polarization
- Other advance surface polishing techniques
- Influence of imperfections
 - lower reflectivity,
 - broader multilayer reflectivity curve,
 - diffuse scattering
- Radiation damages
- Standing waves

On-going developments

- Mirror and multilayers for handling much more coherent X-ray beam
 - slope error < 0.1 μ rad, roughness < 0.05 nm
 - fabrication and characterization
- Nanometer focusing optics
- Multilayers with shorter period
- Stable mount, tables and support

Acknowledgements

Dr. C. Morawe, European Synchrotron Radiation Facility

Prof. Y. Yamauchi, Osaka Univ.

Dr. T. Mochizuki , SPring-8

Dr. T. Hatano, Tohoku Univ.

Prof. M. Nomura, Photon Factory

Dr. T. Uruga, SPring-8

Dr. Y. Higashi, KEK

Dr. M. Suzuki, SPring-8

Dr. Hirono, SPring-8

CXRO_ALS web site: “X-ray Interactions with Matter”
http://henke.lbl.gov/optical_constants